Available online at www.sciencedirect.com
SCIENCE DIRECT®
Journal of Sound and Vibration 280 (2005) 263–287
JOURNAL OF SOUND AND VIBRATION
www.elsevier.com/locate/jsvi

An analysis of a vibratory angular-rate gyroscope using polarized piezoceramic bimorph plates. Part 1: derivation of variational equations in the absence of angular velocity

Jongwon Seok*, H.F. Tiersten, H.A. Scarton

Department of Mechanical, Aerospace and Nuclear Engineering, Rensselaer Polytechnic Institute, 110 8th Street, Troy, NY 12180-3590, USA

Received 16 October 2002; accepted 4 December 2003

Abstract

A variational equation is derived for the in-plane and out-of-plane motions of a configuration composed of two rectangular and annular sector piezoceramic bimorph plates arranged in the shape of one half of a single tuning fork. The required variational equation for the structure is obtained by means of a low order expansion in the three-dimensional variational equation. The elements that connect any of the two bimorph plates, which are at right angles with respect to each other, are modelled as rigid bodies in the continuity conditions at the interface edges of the connected bimorphs.

1. Introduction

The conventional angular-rate gyroscope, based on the conservation of angular momentum of a spinning flywheel, is commonly used in vehicles where size is of little concern. However, for many recent applications, such an angular-rate gyroscope is too expensive, too large, and has a relatively short lifetime determined by the limited life of the rotating sensor devices that wear out significantly faster than the associated electronics.

The concept of a vibratory angular-rate gyroscope was first developed in the middle of the 19th century. In the mid-19th century Leon Foucault [1] developed the underlying theory of rotation sensing, culminating in his pendulum, which calculates the rotation of the earth and thus the period with amazing accuracy. In the middle of the twentieth century, the Sperry Gyroscope

*Corresponding author. Currently: Assistant Professor, School of Mechanical Engineering, College of Engineering, Chung-Ang University, 221, Heukseok-Dong, Dongjak-Gu, Seoul 156-756, Korea. Tel.: +82-31-215-3319; fax: +82-31-215-3319.

E-mail address: seokj@alum.rpi.edu (J. Seok).

0022-460X/$ - see front matter © 2004 Elsevier Ltd. All rights reserved.
doi:10.1016/j.jsv.2003.12.030

Company developed a two-arm tuning fork gyroscope called the Gyrotron as the first successful, artificial vibrating angular-rate sensor [2]. The drive arm contains a magnetic actuator to which an alternating current is applied, causing the material to change shape in an oscillatory manner. The detection sensor is placed on the detection arm in the direction perpendicular to the drive arm. Subject to a constant rotation-rate Ω about the longitudinal axis of the tuning fork, the Coriolis force causes out of plane motion proportional to Ω. This Coriolis force is detected by the detection sensor, which produces a current or a voltage proportional to the angular velocity.

In the 1960s, General Electric replaced the magnetic actuation of the Gyrotron with piezoelectric means in their VYRO [3], in which the in-plane opposing vibratory motion is used to drive the system and the resulting out-of-plane opposing vibrational motion is picked up to measure the angular-rate. Advancement of materials along with the improved manufacturability of polarized ceramics in the 1980s initiated the miniaturization of sensor devices [4]. Watson [5] invented a modification of the common rectangular cross-section tuning fork gyroscope, which has separate driving and detecting tines oriented at right angles relative to each other on the same leg, as treated in this work.

Kudo et al. [6] built and measured Watson's tuning fork gyroscope [5] made of piezoelectric material,[1] much as the configuration treated in this work.[2] In the same work, they also perform a finite element calculation[3] and find a point of zero displacement for support. In addition they [7] built and measured a more conventional double-ended tuning fork gyroscope made of piezoelectric material (see footnote 1) and performed a finite element calculation (see footnote 3) and found a point of zero displacement for support. Ulitko [8] has provided an analytical treatment of a vibratory gyroscope with bimorph beams in the shape of a tuning fork, even though he refers to experimental work [6,7] that employs piezoelectric plates as tines. In the analysis he uses classical Bernoulli–Euler beam theory for both the straight and curved parts, from which he calculates the sensitivity.

In this work, a vibratory gyroscope with bimorph plates arranged in the shape of one half[4] of a tuning fork composed of two cross-jointed bimorph plates connected to an annular sector plate is analyzed. Although some good analytical work on the bimorph exists in the literature [9,10], it is simpler and clearer to obtain the lowest order one-dimensional electrostatic equations for the bimorph plates directly from the three-dimensional equations because the electric field points only in the thin direction of the bimorph plates. The basic configuration of Watson's tuning fork gyroscope [5] is employed for the tines, which have two thin exciting and detecting piezoceramic plates oriented at right angles on one tine. However, in the case treated here the piezoceramic plates are bimorphs and the size is about one-sixth of that built and measured in Ref. [6]. Here a semi-analytic treatment is employed, in which the vibrating bimorph elements are treated as plates, which they are, rather than beams. However, it should be noted that the configuration of the bimorph tuning fork gyroscope treated in this work has not, as yet, been fabricated.

[1] In both works [6,7], the authors do not specify the piezoelectric material or the placement of the electrodes. However, it is likely that they used polarized piezoceramic bimorphs.

[2] The connecting base in the case of Watson's configuration used in Ref. [6] is rectangular, whereas the equivalent element in the case treated in this work is cylindrical.

[3] They make purely elastic displacement calculations and no electrical quantities are calculated in Refs. [6,7]. However, they do measure the appropriate electrical quantities.

[4] Only half of the tuning fork need be treated because of the symmetry of the configuration.

The procedure used in this work employs a modification of Hamilton's principle within the framework of two-dimensional plate theory, for both out-of-plane and in-plane motions of rectangular and annular sector plates, from which appropriate variational equations are obtained. The free flexural vibration problem for a thin elastic[5] cantilever plate has been treated [11] using the variational approximation procedure employed in this work. In the variational approximation procedure used in Ref. [11], the differential equation and edge conditions on both sides of the width are satisfied exactly and the edge conditions at the free and fixed edges are satisfied variationally. Since the variational equation for plates in which all conditions, i.e., those of both natural and constraint type, arise as natural conditions is not readily available, we first derive the two-dimensional variational equation with all natural conditions for the flexural vibrations of thin plates from the existing three-dimensional formulation. This is done by making a low order expansion of the displacement in the thickness co-ordinate and integrating through the thickness in the manner of Mindlin [12]. The exact solution of the differential equations and free edge conditions on opposite faces yields dispersion curves. We take up to a certain number of these solutions represented by the dispersion curves in what remains of the variational equation with all natural conditions to obtain a system of linear inhomogeneous algebraic equations, from which calculations are performed. By means of the same type of variational approximation procedure, the free vibration problem of cantilevered rectangular plates in-plane stress has been treated [13] for the in-plane motion of the plate. In essentially the same manner, the free vibration problem of the cantilevered annular sector plate has been treated for the flexural motion [14] and in-plane motion [15].

2. Development of variational equations

2.1. Three-dimensional variational equation for a linear piezoelectric continuum

For a holonomic system [16], Hamilton's principle can be stated as follows [17]:

$$\delta \int_{t_0}^{t} L \, \mathrm{d}t + \int_{t_0}^{t} \delta W \, \mathrm{d}t = 0, \tag{1}$$

where L is the Lagrangian given by $L = T - V$ and δW is the virtual work done by the non-conservative forces, T and V represent the kinetic and the potential energies of the system, respectively. It has been shown that the variational equation of linear piezoelectricity for infinitesimal strain in a volume V bounded by a surface S may be written in the form [18]

$$\aleph_m + \aleph_e = 0, \tag{2}$$

[5] Since the bimorph is thin, it is shown in Section 2.5 that the purely elastic solutions obtained in the earlier work on free vibrations apply to the piezoelectric case treated in this work provided only that the flexural constants are modified by the influence of the piezoelectric coupling as shown in Eqs. $(43)_2$ and $(43)_3$. In the case of in-plane motion the influence of the piezoelectric coupling cancels in the bimorph. This is a consequence of the fact that the electric field points only in the thin direction between electrodes, which enables the electrical portion of the variational equation to be ignored in this work.

where $\aleph_m$ and $\aleph_e$ denote, respectively, the mechanical and electrical parts of the variational equation, and are defined by

$$\aleph_m = \int_{t_0}^{t} \mathrm{d}t \left[\int_V (\tau_{ij,i} - \rho \ddot{u}_j) \delta u_j \, \mathrm{d}V + \int_S (\bar{t}_j - n_i \tau_{ij}) \delta u_j \, \mathrm{d}S \right], \tag{3}$$

$$\aleph_e = \int_{t_0}^{t} \mathrm{d}t \left[\int_V D_{i,i} \delta\varphi \, \mathrm{d}V - \int_S (\bar{\sigma} + n_i D_i) \delta\varphi \, \mathrm{d}S \right], \tag{4}$$

in which we have introduced indicial notation and employed the conventions that repeated tensor indices are to be summed, and a comma followed by an index denotes partial differentiation with respect to a space co-ordinate and the symbols $\rho, u_j, \tau_{ij}, \bar{t}_j$ and n_i denote the reference mass density, the mechanical displacement vector, the stress tensor, the prescribed surface traction vector and the unit outward normal vector, respectively, and the symbols D_i, φ and $\bar{\sigma}$ denote the electric displacement vector, the electric potential and the prescribed surface charge, respectively. In Eq. (3) we have introduced the convention that a dot over a variable denotes partial differentiation with respect to time.

In addition, the strain–displacement relations, quasistatic electric field–electric scalar potential relations, and the linear piezoelectric constitutive equations required in this description may be written in the form

$$\varepsilon_{kl} = \tfrac{1}{2}(u_{k,l} + u_{l,k}), \quad E_k = -\varphi_{,k}, \tag{5,6}$$

$$\tau_{ij} = c^E_{ijkl} \varepsilon_{kl} - e_{kij} E_k, \quad D_i = e_{ikl} \varepsilon_{kl} + \varepsilon^S_{ik} E_k, \tag{7,8}$$

where E_k is the electric field. As a consequence of footnote 5, the electrical portion of the variational equation need not be treated in this work. Consequently, only the mechanical portion of the variational equation for the bimorph plate is treated in the subsequent sections. Since the electric field points only in the thin direction between the electrodes of the bimorph, the electrical behavior is treated directly in the differential equations in Sections 2.5 and 2.6.

2.2. Description of the gyroscope in the shape of half of a tuning fork

Consider a system consisting of three bimorph structures with mutually orthogonal orientations, in which each of the bimorph elements is fully covered with infinitesimally thin electrodes on top and bottom surfaces, and at the interface between the two layers of the bimorph. The tuning fork contains the following three elements: one end of an annular sector plate is fixed at a rigid wall and the other end is attached to one end of a rectangular plate, which is the sensing plate of the system, by means of a connecting piece, which is employed to ease the stress concentration at the junction. On the other end the rectangular plate is attached to another rectangular plate, which is the actuating plate, with a 90° difference in orientation by means of another connecting piece. Fig. 1(a) shows the schematic three-dimensional shape of this tuning fork system where the geometric symbols $\overset{(n)}{V}$, $n = 1, 2$ and 3, represent the volume of the nth element, $2l, 2b$ and $2h$ represent the length, width and thickness of the rectangular plates, respectively, R_i, R_o and t_c represent the inner and outer radii of the annular sector plate and the thickness of the connecting pieces, respectively. Fig. 1(b) shows the three local co-ordinate systems

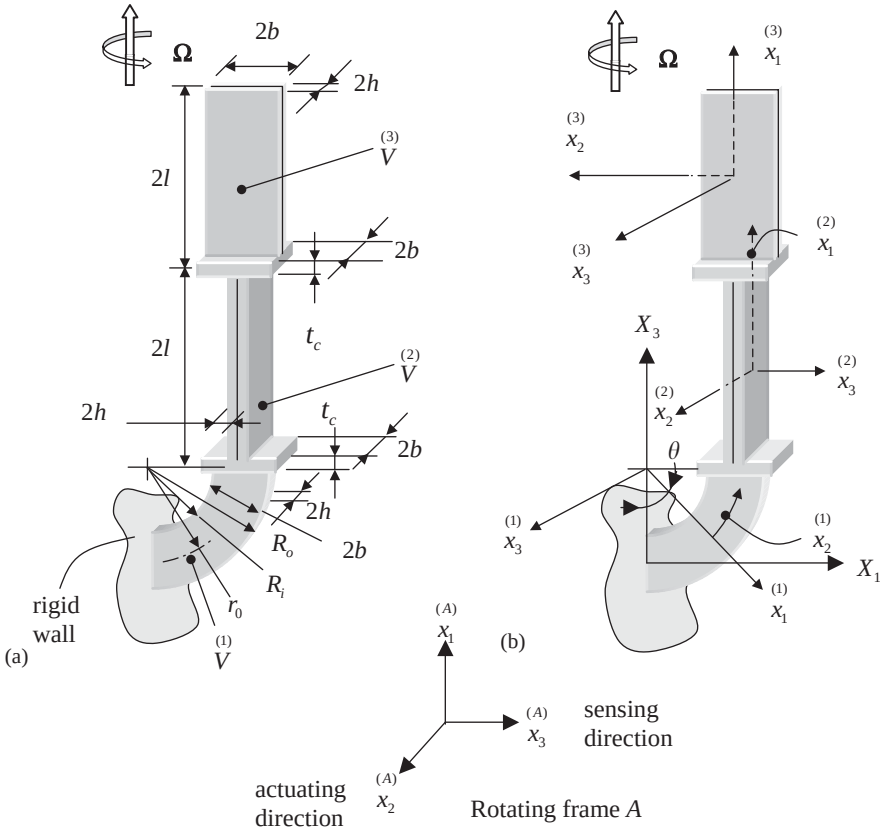

Fig. 1. Three-dimensional view of tuning fork systems: (a) with geometric symbols, (b) with local co-ordinate systems.

located at the center of each part. In Fig. 1(b) we have employed a cylindrical co-ordinate system $(\overset{(1)}{x}_1, \overset{(1)}{x}_2, \overset{(1)}{x}_3) = (r, \theta, z)$ for the annular sector plate and rectangular Cartesian co-ordinate system $(\overset{(m)}{x}_1, \overset{(m)}{x}_2, \overset{(m)}{x}_3)$, $m = 2,\ 3$ for the rectangular plates. The useful motions of the rectangular plates are in the thin directions of the plate. Hence, in accordance with Fig. 1(b) and the diagram of the rotating frame, the $\overset{(A)}{x}_2$ and $\overset{(A)}{x}_3$ directional motions in the rotating frame A will, respectively, be mentioned as the *actuating motion* and the *sensing motion* hereafter.

2.3. *Mechanical part of the variational equation for the actuating motion of the system without superposed angular velocity*

The form of the variational principle for the configuration shown in Fig. 2 is given in Eq. (6.44) of Ref. [19], which is reproduced here for completeness:

$$\int_{t_0}^{t} \mathrm{d}t \sum_{m=1}^{2} \left[\int_{\overset{(m)}{V}} \left(\overset{(m)}{\tau}_{kl,k} - \overset{(m)}{\rho}\, \overset{(m)}{\ddot{u}}_l \right) \delta \overset{(m)}{u}_l \, \mathrm{d}V + \int_{\overset{(m)}{S_N}} \left(\overset{(m)}{\bar{t}}_l - \overset{(m)}{n}_k \overset{(m)}{\tau}_{kl} \right) \delta \overset{(m)}{u}_l \, \mathrm{d}S \right.$$

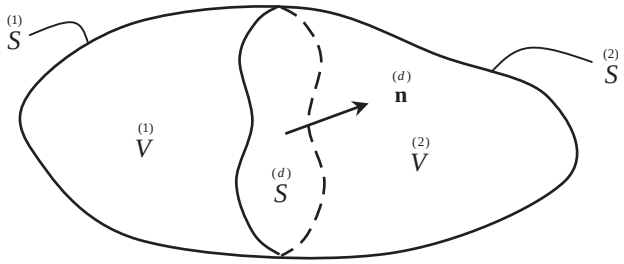

Fig. 2. Diagram of a bounded region containing an internal surface of discontinuity.

$$+\int_{\substack{(m)\\S_C}} \overset{(m)}{n}_k \left(\overset{(m)}{u}_l - \overset{(m)}{\bar{u}}_l\right)\delta\,\overset{(m)}{\tau}_{kl}\,\mathrm{d}S + \int_{t_0}^{t}\mathrm{d}t\int_{\substack{(d)\\S}} \overset{(d)}{n}_k \frac{1}{2}\left[\left(\overset{(2)}{\tau}_{kl} - \overset{(1)}{\tau}_{kl}\right)\left(\delta\,\overset{(1)}{u}_l + \delta\,\overset{(2)}{u}_l\right)\right.$$

$$\left.+\left(\overset{(1)}{u}_l - \overset{(2)}{u}_l\right)\left(\delta\,\overset{(1)}{\tau}_{kl} + \delta\,\overset{(2)}{\tau}_{kl}\right)\right]\mathrm{d}S = 0, \tag{9}$$

where $\overset{(m)}{S}_N, \overset{(m)}{S}_C$ denote the portion of the mth surface on which natural- and constraint-type conditions are prescribed, respectively, $\overset{(d)}{S}$ stands for the surface of discontinuity separating region 1 from region 2, and $\overset{(d)}{n}_k$ denotes the unit normal to the surface of discontinuity directed from region 1 to region 2. Since the gyroscopic system shown in Fig. 1 is composed of three elements with two interface surfaces of discontinuity, Eq. (9) will be extended and specialized to obtain the variational equations required for the description of the system.

For the convenience of the derivation, the symbols for the displacements of the elements are denoted differently depending on the numbering of the elements 1, 2, 3 and direction of vibration: The symbol $\overset{(m)}{w}$ $(m = 2, 3)$ denotes the displacement of the flexural motion of the rectangular plate m in the $\overset{(m)}{x}_3$ direction, $\overset{(2)}{u}_1^{(0)}, \overset{(2)}{u}_2^{(0)}$ stand for the displacements of the in-plane motion of the rectangular plate 2 in the $\overset{(2)}{x}_1$ and $\overset{(2)}{x}_2$ directions, respectively, and the symbol $\overset{(1)}{v}$ denotes the displacement of the flexural motion of the annular sector plate 1 in the $\overset{(1)}{x}_3 = (\overset{(1)}{z})$ direction. Here, each element can be identified from the superscript located at the top-middle of each symbol. In the sequel the symbols M and J with a two-numbered superscript enclosed in the parenthesis located in the middle of each symbol, respectively, stand for the connecting pieces' masses and the mass moment of inertia about two principle axes in the plane of the plate and J_t, the mass moment of inertia about the principle axis normal to the piece. In this work, as in the earlier works [11, 13–15] the two thin plates and the annular sector plate are very accurately treated in classical flexure for the out-of-plane motion and in-plane stress for the in-plane motion. Since the three

thin plates are treated as stated and are joined at right angles through relatively stiff connecting elements, the continuity conditions at the junction must be taken as single point conditions on the average of the flexural and plane stress quantities over each plate at each junction. On account of this, the relatively stiff connecting pieces are automatically modelled as rigid bodies. To represent an equivalent single point quantity a carat (^) is placed over each symbol. It is to be noted that since the plate equations are employed before the averages at the interfaces are taken, Kirchhoff's integration by parts for the twisting moment addition to the shear equation and the corner condition have been obtained and are retained as part of the interface point condition.

From Eq. (16) of Ref. [11] and Eq. (9), the mechanical part of the variational equation for the actuation motion may be written in the form

$$T_1^{IA} + T_2^{IA} + T_3^{IA} = 0, \tag{10}$$

where

$$\begin{aligned} T_1^{IA} \doteq \int_{t_0}^{t} \mathrm{d}t \Bigg[\Bigg[\int_{\overset{(1)}{S}} \mathrm{d}S \Bigg[& \left\{ \overset{(1)}{\tau}{}^{(0)}_{rz,r} + \frac{\overset{(1)}{\tau}{}^{(0)}_{\theta z,\theta} + \overset{(1)}{\tau}{}^{(0)}_{rz}}{r} - 2\rho h \overset{(1)}{\ddot{v}} \right\} \delta \overset{(1)}{v} \\ & + \left\{ \overset{(1)}{\tau}{}^{(1)}_{rr,r} + \frac{\overset{(1)}{\tau}{}^{(1)}_{r\theta,\theta}}{r} + \frac{\overset{(1)}{\tau}{}^{(1)}_{rr} - \overset{(1)}{\tau}{}^{(1)}_{\theta\theta}}{r} - \overset{(1)}{\tau}{}^{(0)}_{rz} \right\} \delta \overset{(1)}{u}{}^{(1)}_{r} \\ & + \left\{ \overset{(1)}{\tau}{}^{(1)}_{r\theta,r} + \frac{1}{r} \left(\overset{(1)}{\tau}{}^{(1)}_{\theta\theta,\theta} + 2\overset{(1)}{\tau}{}^{(1)}_{r\theta} \right) - \overset{(1)}{\tau}{}^{(0)}_{\theta z} \right\} \delta \overset{(1)}{u}{}^{(1)}_{\theta} \Bigg] \\ & + \int_{\overset{(2)}{S}} \mathrm{d}S \left(\overset{(2)}{\tau}{}^{(0)}_{ab,a} - 2\rho h \overset{(2)}{\ddot{u}}{}^{(0)}_{b} \right) \delta \overset{(2)}{u}{}^{(0)}_{b} \\ & + \int_{\overset{(2)}{S}} \mathrm{d}S \left\{ \left(\overset{(2)}{\tau}{}^{(0)}_{a3,a} - 2\rho h \overset{(2)}{\ddot{w}} \right) \delta \overset{(2)}{w} + \left(\overset{(2)}{\tau}{}^{(1)}_{ab,a} - \overset{(2)}{\tau}{}^{(0)}_{3b} \right) \delta \overset{(2)}{u}{}^{(1)}_{b} \right\} \\ & + \int_{\overset{(3)}{S}} \mathrm{d}S \left\{ \left(\overset{(3)}{\tau}{}^{(0)}_{a3,a} - 2\rho h \overset{(3)}{\ddot{w}} \right) \delta \overset{(3)}{w} + \left(\overset{(3)}{\tau}{}^{(1)}_{ab,a} - \overset{(3)}{\tau}{}^{(0)}_{3b} \right) \delta \overset{(3)}{u}{}^{(1)}_{b} \right\} \Bigg] \Bigg], \end{aligned} \tag{11a}$$

$$\begin{aligned} T_2^{IA} \doteq \int_{t_0}^{t} \mathrm{d}t \Bigg[\Bigg[& - \int_{-\Theta}^{\Theta} \mathrm{d}\overset{(1)}{x}_2 \left[r \left\{ \left(\overset{(1)}{\tau}{}^{(0)}_{rz} + \frac{\overset{(1)}{\tau}{}^{(1)}_{r\theta,\theta}}{r} \right) \delta \overset{(1)}{v} - \overset{(1)}{\tau}{}^{(1)}_{rr} \delta \overset{(1)}{\vartheta} \right\} \right]_{\overset{(1)}{x}_1 = R_i}^{\overset{(1)}{x}_1 = R_o} \\ & - \int_{-l}^{l} \mathrm{d}\overset{(2)}{x}_1 \left[\overset{(2)}{\tau}{}^{(0)}_{21} \delta \overset{(2)}{u}{}^{(0)}_{1} + \overset{(2)}{\tau}{}^{(0)}_{22} \delta \overset{(2)}{u}{}^{(0)}_{2} \right]_{\overset{(2)}{x}_2 = -b}^{\overset{(2)}{x}_2 = b} \end{aligned}$$

$$
\begin{aligned}
&- \int_{-l}^{l} \mathrm{d}\overset{(2)}{x}_1 \left[\left(\overset{(2)}{\tau}{}^{(0)}_{23} + \overset{(2)}{\tau}{}^{(1)}_{21,1} \right) \delta \overset{(2)}{w} - \overset{(2)}{\tau}{}^{(1)}_{22}\, \delta \overset{(2)}{\theta}_t \right]_{\overset{(2)}{x}_2=-b}^{\overset{(2)}{x}_2=b} \\
&- \int_{-l}^{l} \mathrm{d}\overset{(3)}{x}_1 \left[\left(\overset{(3)}{\tau}{}^{(0)}_{23} + \overset{(3)}{\tau}{}^{(1)}_{21,1} \right) \delta \overset{(3)}{w} - \overset{(3)}{\tau}{}^{(1)}_{22}\, \delta \overset{(3)}{\theta}_t \right]_{\overset{(3)}{x}_2=-b}^{\overset{(3)}{x}_2=b} \Bigg] \Bigg], \qquad (11b)
\end{aligned}
$$

$$
\begin{aligned}
T_3^{IA} \doteq \int_{t_0}^{t} \mathrm{d}t \Bigg[\Bigg[&- \int_{R_i}^{R_o} \mathrm{d}\overset{(1)}{x}_1 \left[\left(\overset{(1)}{\tau}{}^{(0)}_{\theta z} + \overset{(1)}{\tau}{}^{(1)}_{\theta r,r} \right) \delta \overset{(1)}{v} - \overset{(1)}{\tau}{}^{(1)}_{\theta\theta}\, \delta \overset{(1)}{\upsilon} \right]_{\overset{(1)}{x}_2=\Theta} \\
&- \int_{R_i}^{R_o} \mathrm{d}\overset{(1)}{x}_1 \left[\overset{(1)}{v}\, \delta \overset{(1)}{\tau}{}^{(0)}_{\theta z} - \overset{(1)}{\vartheta}\, \delta \overset{(1)}{\tau}{}^{(1)}_{r\theta} \right]_{\overset{(1)}{x}_2=-\Theta} \\
&- \left[\overset{(1)}{\tau}{}^{(1)}_{r\theta}\, \delta \overset{(1)}{v} \right]_{\overset{(1)}{x}_1=R_i,\overset{(1)}{x}_2=-\Theta}^{\overset{(1)}{x}_1=R_o,\overset{(1)}{x}_2=-\Theta} + 2 \left[\overset{(1)}{\tau}{}^{(1)}_{r\theta}\, \delta \overset{(1)}{v} \right]_{\overset{(1)}{x}_1=R_i,\overset{(1)}{x}_2=\Theta}^{\overset{(1)}{x}_1=R_o,\overset{(1)}{x}_2=\Theta} \\
&- \int_{-b}^{b} \mathrm{d}\overset{(2)}{x}_2 \left[\overset{(2)}{\tau}{}^{(0)}_{11}\, \delta \overset{(2)}{u}{}^{(0)}_1 + \overset{(2)}{\tau}{}^{(0)}_{12}\, \delta \overset{(2)}{u}{}^{(0)}_2 \right]_{\overset{(2)}{x}_1=-l}^{\overset{(2)}{x}_1=l} \\
&- \int_{-b}^{b} \mathrm{d}\overset{(2)}{x}_2 \left[\left(\overset{(2)}{\tau}{}^{(0)}_{13} + \overset{(2)}{\tau}{}^{(1)}_{12,2} \right) \delta \overset{(2)}{w} - \overset{(2)}{\tau}{}^{(1)}_{11}\, \delta \overset{(2)}{\phi} \right]_{\overset{(2)}{x}_1=-l}^{\overset{(2)}{x}_1=l} \\
&- 2 \left[\overset{(2)}{\tau}{}^{(1)}_{12}\, \delta \overset{(2)}{w} \right]_{\overset{(2)}{x}_1=-l,\overset{(2)}{x}_2=-b}^{\overset{(2)}{x}_1=-l,\overset{(2)}{x}_2=b} + 2 \left[\overset{(2)}{\tau}{}^{(1)}_{12}\, \delta \overset{(2)}{w} \right]_{\overset{(2)}{x}_1=l,\overset{(2)}{x}_2=-b}^{\overset{(2)}{x}_1=l,\overset{(2)}{x}_2=b} \\
&- \int_{-b}^{b} \mathrm{d}\overset{(3)}{x}_2 \left[\left(\overset{(3)}{\tau}{}^{(0)}_{13} + \overset{(3)}{\tau}{}^{(1)}_{12,2} \right) \delta \overset{(3)}{w} - \overset{(3)}{\tau}{}^{(1)}_{11}\, \delta \overset{(3)}{\phi} \right]_{\overset{(3)}{x}_1=-l}^{\overset{(3)}{x}_1=l} \\
&- 2 \left[\overset{(3)}{\tau}{}^{(1)}_{12}\, \delta \overset{(3)}{w} \right]_{\overset{(3)}{x}_1=-l,\overset{(3)}{x}_2=-b}^{\overset{(3)}{x}_1=-l,\overset{(3)}{x}_2=b} + 2 \left[\overset{(3)}{\tau}{}^{(1)}_{12}\, \delta \overset{(3)}{w} \right]_{\overset{(3)}{x}_1=l,\overset{(3)}{x}_2=-b}^{\overset{(3)}{x}_1=l,\overset{(3)}{x}_2=b}
\end{aligned}
$$

$$
-\frac{\overset{(1,2)}{M}}{2}\left\{\left[\overset{(1)}{\ddot{v}}\ \delta\ \overset{(1)}{\hat{v}}\right]_{\overset{(1)}{x_2}=\Theta}+\left[\overset{(2)}{\ddot{u}_2^{(0)}}\ \delta\ \overset{(2)}{\hat{u}_2^{(0)}}\right]_{\overset{(2)}{x_1}=-l}\right\}
$$

$$
-\frac{\overset{(1,2)}{J}}{2}\left\{\left[\overset{(1)}{\ddot{v}}\ \delta\ \overset{(1)}{\hat{v}}\right]_{\overset{(1)}{x_2}=\Theta}+\left[\overset{(2)}{\ddot{\psi}}\ \delta\ \overset{(2)}{\hat{\psi}}\right]_{\overset{(2)}{x_1}=-l}\right\}
$$

$$
-\frac{\overset{(1,2)}{J_t}}{2}\left\{\left[\overset{(1)}{\ddot{\vartheta}}\ \delta\ \overset{(1)}{\hat{\vartheta}}\right]_{\overset{(1)}{x_2}=\Theta}+\left[\overset{(2)}{\ddot{\theta}_t}\ \delta\ \overset{(2)}{\hat{\theta}_t}\right]_{\overset{(2)}{x_1}=-l}\right\}
$$

$$
-\frac{\overset{(2,3)}{M}}{2}\left\{\left[\overset{(2)}{\ddot{u}_2^{(0)}}\ \delta\ \overset{(2)}{\hat{u}_2^{(0)}}\right]_{\overset{(2)}{x_1}=l}+\left[\overset{(3)}{\ddot{w}}\ \delta\ \overset{(3)}{\hat{w}}\right]_{\overset{(3)}{x_1}=-l}\right\}
$$

$$
-\frac{\overset{(2,3)}{J}}{2}\left\{\left[\overset{(2)}{\ddot{\psi}}\ \delta\ \overset{(2)}{\hat{\psi}}\right]_{\overset{(2)}{x_1}=l}+\left[\overset{(3)}{\ddot{\phi}}\ \delta\ \overset{(3)}{\hat{\phi}}\right]_{\overset{(3)}{x_1}=-l}\right\}
$$

$$
-\frac{\overset{(2,3)}{J_t}}{2}\left\{\left[\overset{(2)}{\ddot{\theta}_t}\ \delta\ \overset{(2)}{\hat{\theta}_t}\right]_{\overset{(2)}{x_1}=l}+\left[\overset{(3)}{\ddot{\theta}_t}\ \delta\ \overset{(3)}{\hat{\theta}_t}\right]_{\overset{(3)}{x_1}=-l}\right\}
$$

$$
+\delta\left[\overset{(1,2)}{\lambda_d}\left\{\left[\overset{(1)}{\hat{v}}\right]_{\overset{(1)}{x_2}=\Theta}-\left[\overset{(2)}{\hat{u}_2^{(0)}}\right]_{\overset{(2)}{x_1}=-l}\right\}\right]+\delta\left[\overset{(1,2)}{\lambda_s}\left\{\left[\overset{(1)}{\hat{v}}\right]_{\overset{(1)}{x_2}=\Theta}-\left[\overset{(2)}{\hat{\psi}}\right]_{\overset{(2)}{x_1}=-l}\right\}\right]
$$

$$
+\delta\left[\overset{(1,2)}{\lambda_t}\left\{\left[\overset{(1)}{\hat{\vartheta}}\right]_{\overset{(1)}{x_2}=\Theta}+\left[\overset{(2)}{\hat{\theta}_t}\right]_{\overset{(2)}{x_1}=-l}\right\}\right]+\delta\left[\overset{(2,3)}{\lambda_d}\left\{\left[\overset{(2)}{\hat{u}_2^{(0)}}\right]_{\overset{(2)}{x_1}=l}-\left[\overset{(3)}{\hat{w}}\right]_{\overset{(3)}{x_1}=-l}\right\}\right]
$$

$$
+\delta\left[\overset{(2,3)}{\lambda_s}\left\{\left[\overset{(2)}{\hat{\psi}}\right]_{\overset{(2)}{x_1}=l}-\left[\overset{(3)}{\hat{\phi}}\right]_{\overset{(3)}{x_1}=-l}\right\}\right]+\delta\left[\overset{(2,3)}{\lambda_t}\left\{\left[\overset{(2)}{\hat{\theta}_t}\right]_{\overset{(2)}{x_1}=l}-\left[\overset{(3)}{\hat{\theta}_t}\right]_{\overset{(3)}{x_1}=-l}\right\}\right]\Bigg]\Bigg]\Bigg], \tag{11c}
$$

in which we employ the convention that $[f(x)]_{x=a}^{x=b} = f(b) - f(a)$, $[g(x)]_{x=a} = g(a)$, the symbol λ represents the Lagrange multipliers, and

$$\overset{(m)}{\tau}{}_{ij}^{(n)} = \int_{-h}^{h} \overset{(m)}{\tau}_{ij}\, \overset{(m)}{x}_3^n \, \mathrm{d}\overset{(m)}{x}_3, \quad \overset{(m)}{u}_j = \sum_{n=0}^{N} \overset{(m)}{u}_j^{(n)}\, \overset{(m)}{x}_3, \quad m = 1,2 \text{ and } 3,$$

$$N = \begin{cases} 1 & \text{for } j = 1,2, \\ 2 & \text{for } j = 3, \end{cases} \tag{12}$$

$$\overset{(1)}{v} \doteq \overset{(1)}{u}_z^{(0)}, \quad \overset{(1)}{v} \doteq \frac{\overset{(1)}{v}_{,\theta}}{r}, \quad \overset{(1)}{\vartheta} \doteq \overset{(1)}{v}_{,r}, \quad \overset{(2)}{\psi} \doteq \frac{1}{2}\left(\overset{(2)}{u}_{2,1}^{(0)} - \overset{(2)}{u}_{1,2}^{(0)}\right), \quad \overset{(m)}{\theta}_t \doteq \overset{(m)}{w}_{,2}, \quad \overset{(m)}{w} \doteq \overset{(m)}{u}_3^{(0)},$$

$$m = 2,3, \quad \overset{(3)}{\phi} \doteq \overset{(3)}{w}_{,1} \tag{13}$$

and the notational conventions explained in Section 2 of Refs. [11,14] are employed and are to be understood. In Eq. (11c) virtual work terms have been introduced to account for the rigid body behavior of the connecting pieces. Note that T_1^{IA}, T_2^{IA} and T_3^{IA} defined in Eqs. (11a)–(11c) are the terms of the variational equation for the large surfaces, free opposing edges and interface and extreme edges of the structure for the actuating directional vibration in the absence of angular velocity, respectively, where the edge conditions on the free opposing edges are satisfied exactly to obtain dispersion relations in the treatment. Also note that the bending moments $\overset{(3)}{\tau}{}_{11}^{(1)}$ and $\overset{(3)}{\tau}{}_{22}^{(1)}$ for the actuating flexural motion of the rectangular plate contain the forcing terms induced by the externally applied voltage when the piezoelectric constitutive equations are introduced,[6] as explained in detail in Section 2.5.

To determine the Lagrange multipliers in Eq. (11c), equivalent single point quantities should be defined, which may be written in the form

$$\int_{R_i}^{R_o} \mathrm{d}\overset{(1)}{x}_1 \left[\left(\overset{(1)}{\tau}{}_{\theta z}^{(0)} + \overset{(1)}{\tau}{}_{\theta r,r}^{(1)} \right) \delta \overset{(1)}{v} \right]_{\overset{(1)}{x}_2 = \Theta}$$

[6] In the homogeneous case the dispersion curves are obtained from exact solutions of the differential equations and free conditions on opposite edges for both in-plane and out-of-plane motions in each plate. Since the dispersion curves represent the best solution functions, i.e., require the fewest in number, for obtaining a variational approximation to the solution for the tuning fork bimorph in the inhomogeneous case, we employ these dispersion curves in obtaining the variational approximation in the inhomogeneous case. Inasmuch as the inhomogeneous terms are transformed out of the differential equations into the edge conditions, the differential equations remain homogeneous and, consequently, have been satisfied exactly when the dispersion curves are used. Hence, all differential equation terms, i.e., all surface area terms, in the variational equations vanish and only edge condition terms, i.e., line integral terms, remain. However, since the conditions on the free edges are inhomogeneous, the amplitudes that were obtained from the solutions that satisfied the free edge conditions exactly in the homogeneous case cannot be used to satisfy the conditions on the opposite edges in the inhomogeneous case. In that case the amplitudes must be determined from the inhomogeneous linear algebras obtained from the variational equations that contain only inhomogeneous edge and interface terms. The calculations performed in Part 2 of this work show that extremely rapid convergence is obtained.

$$\doteq \left[\int_{R_i}^{R_o} \left(\overset{(1)}{\tau}{}^{(0)}_{\theta z} + \overset{(1)}{\tau}{}^{(1)}_{\theta r,r} \right) \mathrm{d}\overset{(1)}{x}_1 \cdot \delta \overset{(1)}{\hat{v}} + \int_{R_i}^{R_o} \left(\overset{(1)}{\tau}{}^{(0)}_{\theta z} + \overset{(1)}{\tau}{}^{(1)}_{\theta r,r} \right) (r - r_0)\, \mathrm{d}\overset{(1)}{x}_1 \cdot \delta \overset{(1)}{\hat{\vartheta}} \right]_{\overset{(1)}{x}_2 = \Theta}, \tag{14a}$$

$$\int_{R_i}^{R_o} \mathrm{d}\overset{(1)}{x}_1 \left[\overset{(1)}{\tau}{}^{(1)}_{\theta\theta}\, \delta \overset{(1)}{v} \right]_{\overset{(1)}{x}_2 = \Theta} \doteq \left[\int_{R_i}^{R_o} \overset{(1)}{\tau}{}^{(1)}_{\theta\theta}\, \mathrm{d}\overset{(1)}{x}_1 \cdot \delta \overset{(1)}{\hat{v}} \right]_{\overset{(1)}{x}_2 = \Theta}, \tag{14b}$$

$$\int_{-b}^{b} \mathrm{d}\overset{(2)}{x}_2 \left[\overset{(2)}{\tau}{}^{(0)}_{11}\, \delta \overset{(2)}{u}{}^{(0)}_{1} \right]_{\overset{(2)}{x}_1 = \pm l} \doteq - \left[\int_{-b}^{b} \overset{(2)}{\tau}{}^{(0)}_{11}\, \overset{(2)}{x}_2\, \mathrm{d}\overset{(2)}{x}_2 \cdot \delta \overset{(2)}{\hat{\psi}} \right]_{\overset{(2)}{x}_1 = \pm l}, \tag{14c}$$

$$\int_{-b}^{b} \mathrm{d}\overset{(2)}{x}_2 \left[\overset{(2)}{\tau}{}^{(0)}_{12}\, \delta \overset{(2)}{u}{}^{(0)}_{2} \right]_{\overset{(2)}{x}_1 = \pm l} \doteq \left[\int_{-b}^{b} \overset{(2)}{\tau}{}^{(0)}_{12}\, \mathrm{d}\overset{(2)}{x}_2 \cdot \delta \overset{(2)}{\hat{u}}_2 \right]_{\overset{(2)}{x}_1 = \pm l}, \tag{14d}$$

$$\int_{-b}^{b} \mathrm{d}\overset{(2)}{x}_2 \left[\left(\overset{(2)}{\tau}{}^{(0)}_{13} + \overset{(2)}{\tau}{}^{(1)}_{12,2} \right) \delta \overset{(2)}{w} \right]_{\overset{(2)}{x}_1 = \pm l} \doteq \left[\int_{-b}^{b} \left(\overset{(2)}{\tau}{}^{(0)}_{13} + \overset{(2)}{\tau}{}^{(1)}_{12,2} \right) \overset{(2)}{x}_2\, \mathrm{d}\overset{(2)}{x}_2 \cdot \delta \overset{(2)}{\hat{\theta}}_t \right]_{\overset{(2)}{x}_1 = \pm l}, \tag{14e}$$

$$\begin{aligned} \int_{-b}^{b} \mathrm{d}\overset{(3)}{x}_2 \left[\left(\overset{(3)}{\tau}{}^{(0)}_{13} + \overset{(3)}{\tau}{}^{(1)}_{12,2} \right) \delta \overset{(3)}{w} \right]_{\overset{(3)}{x}_1 = -l} \doteq & \left[\int_{-b}^{b} \left(\overset{(3)}{\tau}{}^{(0)}_{13} + \overset{(3)}{\tau}{}^{(1)}_{12,2} \right) \mathrm{d}\overset{(3)}{x}_2 \cdot \delta \overset{(3)}{\hat{w}} \right. \\ & \left. + \int_{-b}^{b} \left(\overset{(3)}{\tau}{}^{(0)}_{13} + \overset{(3)}{\tau}{}^{(1)}_{12,2} \right) \overset{(3)}{x}_2\, \mathrm{d}\overset{(3)}{x}_2 \cdot \delta \overset{(3)}{\hat{\theta}}_t \right]_{\overset{(3)}{x}_1 = -l}, \end{aligned} \tag{14f}$$

$$\int_{-b}^{b} \mathrm{d}\overset{(3)}{x}_2 \left[\overset{(3)}{\tau}{}^{(1)}_{11}\, \delta \overset{(3)}{\phi} \right]_{\overset{(3)}{x}_1 = -l} \doteq \left[\int_{-b}^{b} \overset{(3)}{\tau}{}^{(1)}_{11}\, \mathrm{d}\overset{(3)}{x}_2 \cdot \delta \overset{(3)}{\hat{\phi}} \right]_{\overset{(3)}{x}_1 = -l}, \tag{14g}$$

where $r_0 = (R_o - R_i)/2$ represents the radius of the center of the annular sector plate. Note that the first and the second terms in the right-hand sides of Eqs. (14a) and (14f), respectively, represent the functionals for the symmetric and antisymmetric modes of the annular sector plate 1 and rectangular plates 3, respectively, for the out-of-plane motion. As stated earlier, Kirchhoff's corner conditions are retained as part of the interface point conditions, and may be defined as

single point quantities in the form

$$\left[\overset{(1)}{\tau}{}^{(1)}_{r\theta}\,\delta\,\overset{(1)}{v}\right]_{\overset{(1)}{x_1}=R_i,R_o,\overset{(1)}{x_2}=\Theta} \doteq \left[\overset{(1)}{\tau}{}^{(1)}_{r\theta}\,\delta\,\overset{(1)}{\hat{v}} + \overset{(1)}{\tau}{}^{(1)}_{r\theta}(r-r_0)\delta\,\overset{(1)}{\hat{\vartheta}}\right]_{\overset{(1)}{x_1}=R_i,R_o,\overset{(1)}{x_2}=\Theta}, \tag{14h}$$

$$\left[\overset{(2)}{\tau}{}^{(1)}_{12}\,\delta\,\overset{(2)}{w}\right]_{\overset{(2)}{x_1}=\pm l,\overset{(2)}{x_2}=\pm b} \doteq \left[\overset{(2)}{\tau}{}^{(1)}_{12}\,\overset{(2)}{x_2}\cdot\delta\,\overset{(2)}{\hat{\theta}_t}\right]_{\overset{(2)}{x_1}=\pm l,\overset{(2)}{x_2}=\pm b}, \tag{14i}$$

$$\left[\overset{(3)}{\tau}{}^{(1)}_{12}\,\delta\,\overset{(3)}{w}\right]_{\overset{(3)}{x_1}=-l,\overset{(3)}{x_2}=\pm b} \doteq \left[\overset{(3)}{\tau}{}^{(1)}_{12}\,\delta\,\overset{(3)}{\hat{w}} + \overset{(3)}{\tau}{}^{(1)}_{12}\,\overset{(3)}{x_2}\cdot\delta\,\overset{(3)}{\hat{\theta}_t}\right]_{\overset{(3)}{x_1}=-l,\overset{(3)}{x_2}=\pm b}, \tag{14j}$$

where the first and the second terms in the right-hand sides of Eqs. (14h) and (14j), respectively, represent the functions for the symmetric and antisymmetric motions of the annular sector plate 1 and the rectangular plates 3, respectively.

Since Lagrange multipliers were used with constraint type conditions in the principle from which Eq. (10) was derived [19], each variation in Eq. (10) is treated as unconstrained [20]. Hence, all the coefficients of the variations in Eq. (10) vanish independently, from which the plate differential equations, edge and corner conditions can be obtained. Substituting the above definitions into the variational Eq. (10) and performing the indicated multiplications in Eq. (10) while solving for the Lagrange multipliers, after utilizing the arbitrariness of the variations of the single point displacements, slopes and rotations, enables us to obtain the equations for the Lagrange multipliers. Note that the Lagrange multipliers are not unique because a single Lagrange multiplier has two different identities on each side of the internal surface of discontinuity. However, in order not to weight one side more than the other, the most appropriate form of the Lagrange multiplier clearly must be obtained by taking the mean of the two Lagrange multipliers on each side [19]. In view of this, the substitutions of Eqs. (14a)–(14j) into Eq. (10) yield the Lagrange multipliers in the form

$$\begin{aligned}\overset{(1,2)}{\lambda_d} = \frac{1}{2}\Bigg[&\left[\int_{R_i}^{R_o}\left(\overset{(1)}{\tau}{}^{(0)}_{\theta z}+\overset{(1)}{\tau}{}^{(1)}_{\theta r,r}\right)\mathrm{d}\,\overset{(1)}{x_1}\right]_{\overset{(1)}{x_2}=\Theta} - \left[\overset{(1)}{\tau}{}^{(1)}_{r\theta}\right]_{\overset{(1)}{x_1}=R_i,\overset{(1)}{x_2}=\Theta}^{\overset{(1)}{x_1}=R_o,\overset{(1)}{x_2}=\Theta} + \left[\int_{-b}^{b}\overset{(2)}{\tau}{}^{(0)}_{12}\,\mathrm{d}\,\overset{(2)}{x_2}\right]_{\overset{(2)}{x_1}=-l}\\ &+\frac{\overset{(1,2)}{M}}{2}\left\{\left[\overset{(1)}{\hat{v}}\right]_{\overset{(1)}{x_2}=\Theta} - \left[\overset{(2)}{\ddot{\hat{u}}}{}^{(0)}_{2}\right]_{\overset{(2)}{x_1}=-l}\right\}\Bigg],\end{aligned} \tag{15a}$$

$$\overset{(1,2)}{\lambda_s} = -\frac{1}{2}\left[\left[\int_{R_i}^{R_o}\overset{(1)}{\tau}{}^{(1)}_{\theta\theta}\,\mathrm{d}\,\overset{(1)}{x_1}\right]_{\overset{(1)}{x_2}=\Theta} + \left[\int_{-b}^{b}\overset{(2)}{\tau}{}^{(0)}_{11}\,\overset{(2)}{x_2}\,\mathrm{d}\,\overset{(2)}{x_2}\right]_{\overset{(2)}{x_1}=-l} - \frac{\overset{(1,2)}{J}}{2}\left\{\left[\overset{(1)}{\ddot{v}}\right]_{\overset{(1)}{x_2}=\Theta} - \left[\overset{(2)}{\ddot{\hat{\psi}}}\right]_{\overset{(2)}{x_1}=-l}\right\}\right], \tag{15b}$$

$$
\begin{aligned}
\overset{(1,2)}{\lambda_t} = \frac{1}{2}\Bigg[& \left[\int_{R_i}^{R_o}\left(\overset{(1)}{\tau}{}^{(0)}_{\theta z}+\overset{(1)}{\tau}{}^{(1)}_{\theta r,r}\right)(r-r_0)\,\mathrm{d}\,\overset{(1)}{x}_1\right]_{\overset{(1)}{x}_2=\Theta} - \left[\overset{(1)}{\tau}{}^{(1)}_{r\theta}(r-r_0)\right]_{\overset{(1)}{x}_1=R_i,\overset{(1)}{x}_2=\Theta}^{\overset{(1)}{x}_1=R_o,\overset{(1)}{x}_2=\Theta} \\
& + \left[\overset{(2)}{\tau}{}^{(1)}_{12}\,\overset{(2)}{x}_2\right]_{\overset{(2)}{x}_1=-l,\overset{(2)}{x}_2=-b}^{\overset{(2)}{x}_1=-l,\overset{(2)}{x}_2=b} \\
& - \left[\int_{-b}^{b}\left(\overset{(2)}{\tau}{}^{(0)}_{13}+\overset{(2)}{\tau}{}^{(1)}_{12,2}\right)\overset{(2)}{x}_2\,\mathrm{d}\,\overset{(2)}{x}_2\right]_{\overset{(2)}{x}_1=-l} + \frac{\overset{(1,2)}{J_t}}{2}\left\{\left[\ddot{\overset{(1)}{\vartheta}}\right]_{\overset{(1)}{x}_2=\Theta} + \left[\ddot{\overset{(2)}{\theta}}_t\right]_{\overset{(2)}{x}_1=-l}\right\}\Bigg],
\end{aligned}
\tag{15c}
$$

$$
\begin{aligned}
\overset{(2,3)}{\lambda_d} = \frac{1}{2}\Bigg[& \left[\int_{-b}^{b}\overset{(2)}{\tau}{}^{(0)}_{12}\,\mathrm{d}\,\overset{(2)}{x}_2\right]_{\overset{(2)}{x}_1=l} + \left[\int_{-b}^{b}\left(\overset{(3)}{\tau}{}^{(0)}_{13}+\overset{(3)}{\tau}{}^{(1)}_{12,2}\right)\mathrm{d}\,\overset{(3)}{x}_2\right]_{\overset{(3)}{x}_1=-l} - \left[\overset{(3)}{\tau}{}^{(1)}_{12}\right]_{\overset{(3)}{x}_1=-l,\overset{(3)}{x}_2=-b}^{\overset{(3)}{x}_1=-l,\overset{(3)}{x}_2=b} \\
& + \frac{\overset{(2,3)}{M}}{2}\left\{\left[\ddot{\overset{(2)}{u}}{}^{(0)}_2\right]_{\overset{(2)}{x}_1=l} - \left[\ddot{\overset{(3)}{w}}\right]_{\overset{(3)}{x}_1=-l}\right\}\Bigg],
\end{aligned}
\tag{15d}
$$

$$
\overset{(2,3)}{\lambda_s} = -\frac{1}{2}\left[\left[\int_{-b}^{b}\overset{(2)}{\tau}{}^{(0)}_{11}\,\overset{(2)}{x}_2\,\mathrm{d}\,\overset{(2)}{x}_2\right]_{\overset{(2)}{x}_1=l} + \left[\int_{-b}^{b}\overset{(3)}{\tau}{}^{(1)}_{11}\,\mathrm{d}\,\overset{(3)}{x}_2\right]_{\overset{(3)}{x}_1=-l} - \frac{\overset{(2,3)}{J}}{2}\left\{\left[\ddot{\overset{(2)}{\psi}}\right]_{\overset{(2)}{x}_1=l} - \left[\ddot{\overset{(3)}{\phi}}\right]_{\overset{(3)}{x}_1=-l}\right\}\right],
\tag{15e}
$$

$$
\begin{aligned}
\overset{(2,3)}{\lambda_t} = \frac{1}{2}\Bigg[& \left[\int_{-b}^{b}\left(\overset{(2)}{\tau}{}^{(0)}_{13}+\overset{(2)}{\tau}{}^{(1)}_{12,2}\right)\overset{(2)}{x}_2\,\mathrm{d}\,\overset{(2)}{x}_2\right]_{\overset{(2)}{x}_1=l} - \left[\overset{(2)}{\tau}{}^{(1)}_{12}\,\overset{(2)}{x}_2\right]_{\overset{(2)}{x}_1=l,\overset{(2)}{x}_2=-b}^{\overset{(2)}{x}_1=l,\overset{(2)}{x}_2=b} \\
& - \left[\overset{(3)}{\tau}{}^{(1)}_{12}\,\overset{(3)}{x}_2\right]_{\overset{(3)}{x}_1=-l,\overset{(3)}{x}_2=-b}^{\overset{(3)}{x}_1=-l,\overset{(3)}{x}_2=b} + \left[\int_{-b}^{b}\left(\overset{(3)}{\tau}{}^{(0)}_{13}+\overset{(3)}{\tau}{}^{(1)}_{12,2}\right)\overset{(3)}{x}_2\,\mathrm{d}\,\overset{(3)}{x}_2\right]_{\overset{(3)}{x}_1=-l} \\
& + \frac{\overset{(2,3)}{J_t}}{2}\left\{\left[\ddot{\overset{(2)}{\theta}}_t\right]_{\overset{(2)}{x}_1=l} - \left[\ddot{\overset{(3)}{\theta}}_t\right]_{\overset{(3)}{x}_1=-l}\right\}\Bigg].
\end{aligned}
\tag{15f}
$$

2.4. Mechanical part of variational equation for the sensing motion of the system without superposed angular velocity

The symbols $\overset{(3)}{u}{}_1^{(0)}$ and $\overset{(3)}{u}{}_2^{(0)}$ are employed for the displacements of the rectangular plate 3 vibrating in the $\overset{(3)}{x}_1$ and $\overset{(3)}{x}_2$ directions, respectively, and $\overset{(1)}{u}{}_r^{(0)}$, $\overset{(1)}{u}{}_\theta^{(0)}$ stand for the displacements of the in-plane motion of the annular sector plate 1 in the $\overset{(1)}{x}_1(=r)$ and $\overset{(1)}{x}_2(=\theta)$ directions, respectively.

From Eq. (16) of Ref. [11] and Eq. (9), the mechanical part of the variational equation for the sensing system may be written the form

$$T_1^{IS} + T_2^{IS} + T_3^{IS} = 0, \tag{16}$$

where

$$\begin{aligned} T_1^{IS} \doteq \int_{t_0}^{t} \mathrm{d}t \Bigg[\Bigg[\int_{\overset{(1)}{S}} \mathrm{d}S \Bigg\{ \Bigg(\overset{(1)}{\tau}{}_{rr,r}^{(0)} + \Bigg\{ \overset{(1)}{\tau}{}_{r\theta,\theta}^{(0)} + \Bigg(\overset{(1)}{\tau}{}_{rr}^{(0)} - \overset{(1)}{\tau}{}_{\theta\theta}^{(0)} \Bigg) \Bigg\} \Big/ r - 2\rho h \, \overset{(1)}{\ddot{u}}{}_r^{(0)} \Bigg) \delta \overset{(1)}{u}{}_r^{(0)} \\ + \Bigg(\frac{\overset{(1)}{\tau}{}_{\theta\theta,\theta}^{(0)}}{r} + \overset{(1)}{\tau}{}_{r\theta,r}^{(0)} + \frac{2}{r} \overset{(1)}{\tau}{}_{r\theta}^{(0)} - 2\rho h \, \overset{(1)}{\ddot{u}}{}_\theta^{(0)} \Bigg) \delta \overset{(1)}{u}{}_\theta^{(0)} \Bigg\} \\ + \int_{\overset{(2)}{S}} \mathrm{d}S \Bigg\{ \Bigg(\overset{(2)}{\tau}{}_{a3,a}^{(0)} - 2\rho h \, \overset{(2)}{\ddot{w}} \Bigg) \delta \overset{(2)}{w} + \Bigg(\overset{(2)}{\tau}{}_{ab,a}^{(1)} - \overset{(2)}{\tau}{}_{3b}^{(0)} \Bigg) \delta \overset{(2)}{u}{}_b^{(1)} \Bigg\} \\ + \int_{\overset{(2)}{S}} \mathrm{d}S \Bigg(\overset{(2)}{\tau}{}_{ab,a}^{(0)} - 2\rho h \, \overset{(2)}{\ddot{u}}{}_b^{(0)} \Bigg) \delta \overset{(2)}{u}{}_b^{(0)} + \int_{\overset{(3)}{S}} \mathrm{d}S \Bigg(\overset{(3)}{\tau}{}_{ab,a}^{(0)} - 2\rho h \, \overset{(3)}{\ddot{u}}{}_b^{(0)} \Bigg) \delta \overset{(3)}{u}{}_b^{(0)} \Bigg] \Bigg], \end{aligned} \tag{17a}$$

$$\begin{aligned} T_2^{IS} \doteq \int_{t_0}^{t} \mathrm{d}t \Bigg[\Bigg[- \int_{-\Theta}^{\Theta} \mathrm{d} \overset{(1)}{x}_2 \Bigg[r \Bigg\{ \overset{(1)}{\tau}{}_{rr}^{(0)} \, \delta \overset{(1)}{u}{}_r^{(0)} + \overset{(1)}{\tau}{}_{r\theta}^{(0)} \, \delta \overset{(1)}{u}{}_\theta^{(0)} \Bigg\} \Bigg]_{\overset{(1)}{x}_1 = R_i}^{\overset{(1)}{x}_1 = R_o} \\ - \int_{-l}^{l} \mathrm{d} \overset{(2)}{x}_1 \Bigg[\Bigg(\overset{(2)}{\tau}{}_{23}^{(0)} + \overset{(2)}{\tau}{}_{21,1}^{(1)} \Bigg) \delta \overset{(2)}{w} - \overset{(2)}{\tau}{}_{22}^{(1)} \, \delta \overset{(2)}{\theta}_t \Bigg]_{\overset{(2)}{x}_2 = -b}^{\overset{(2)}{x}_2 = b} \\ - \int_{-l}^{l} \mathrm{d} \overset{(2)}{x}_1 \Bigg[\overset{(2)}{\tau}{}_{21}^{(0)} \, \delta \overset{(2)}{u}{}_1^{(0)} + \overset{(2)}{\tau}{}_{22}^{(0)} \, \delta \overset{(2)}{u}{}_2^{(0)} \Bigg]_{\overset{(2)}{x}_2 = -b}^{\overset{(2)}{x}_2 = b} - \int_{-l}^{l} \mathrm{d} \overset{(3)}{x}_1 \Bigg[\overset{(3)}{\tau}{}_{21}^{(0)} \, \delta \overset{(3)}{u}{}_1^{(0)} + \overset{(3)}{\tau}{}_{22}^{(0)} \, \delta \overset{(3)}{u}{}_2^{(0)} \Bigg]_{\overset{(3)}{x}_2 = -b}^{\overset{(3)}{x}_2 = b} \Bigg] \Bigg], \end{aligned} \tag{17b}$$

$$
\begin{aligned}
T_3^{IS} \doteq \int_{t_0}^{t} \mathrm{d}t \Bigg[\Bigg[& - \int_{R_i}^{R_o} \mathrm{d}\overset{(1)}{x}_1 \left[\overset{(1)}{\tau}{}^{(0)}_{\theta r}\, \delta \overset{(1)}{u}{}^{(0)}_{r} + \overset{(1)}{\tau}{}^{(0)}_{\theta\theta}\, \delta \overset{(1)}{u}{}^{(0)}_{\theta} \right]_{\overset{(1)}{x}_2=\Theta} \\
& - \int_{R_i}^{R_o} \mathrm{d}\overset{(1)}{x}_1 \left[\overset{(1)}{u}{}^{(0)}_{r}\, \delta \overset{(1)}{\tau}{}^{(0)}_{\theta r} + \overset{(1)}{u}{}^{(0)}_{\theta}\, \delta \overset{(1)}{\tau}{}^{(0)}_{\theta\theta} \right]_{\overset{(1)}{x}_2=-\Theta} \\
& - \int_{-b}^{b} \mathrm{d}\overset{(2)}{x}_2 \left[\left(\overset{(2)}{\tau}{}^{(0)}_{13} + \overset{(2)}{\tau}{}^{(1)}_{12,2} \right) \delta \overset{(2)}{w} - \overset{(2)}{\tau}{}^{(1)}_{11}\, \delta \overset{(2)}{\phi} \right]_{\overset{(2)}{x}_1=-l}^{\overset{(2)}{x}_1=l} \\
& - 2 \left[\overset{(2)}{\tau}{}^{(1)}_{12}\, \delta \overset{(2)}{w} \right]_{\overset{(2)}{x}_1=-l,\overset{(2)}{x}_2=-b}^{\overset{(2)}{x}_1=-l,\overset{(2)}{x}_2=b} + 2 \left[\overset{(2)}{\tau}{}^{(1)}_{12}\, \delta \overset{(2)}{w} \right]_{\overset{(2)}{x}_1=l,\overset{(2)}{x}_2=-b}^{\overset{(2)}{x}_1=l,\overset{(2)}{x}_2=b} \\
& - \int_{-b}^{b} \mathrm{d}\overset{(2)}{x}_2 \left[\overset{(2)}{\tau}{}^{(0)}_{11}\, \delta \overset{(2)}{u}{}^{(0)}_{1} + \overset{(2)}{\tau}{}^{(0)}_{12}\, \delta \overset{(2)}{u}{}^{(0)}_{2} \right]_{\overset{(2)}{x}_1=-l}^{\overset{(2)}{x}_1=l} - \int_{-b}^{b} \mathrm{d}\overset{(3)}{x}_2 \left[\overset{(3)}{\tau}{}^{(0)}_{11}\, \delta \overset{(3)}{u}{}^{(0)}_{1} + \overset{(3)}{\tau}{}^{(0)}_{12}\, \delta \overset{(3)}{u}{}^{(0)}_{2} \right]_{\overset{(3)}{x}_1=-l}^{\overset{(3)}{x}_1=l} \\
& - \frac{\overset{(1,2)}{M}}{2} \left\{ \left[\overset{(1)}{\ddot{u}}{}^{(0)}_{r}\, \delta \overset{(1)}{\hat{u}}{}^{(0)}_{r} + \overset{(1)}{\ddot{u}}{}^{(0)}_{\theta}\, \delta \overset{(1)}{\hat{u}}{}^{(0)}_{\theta} \right]_{\overset{(1)}{x}_2=\Theta} + \left[\overset{(2)}{\ddot{u}}{}^{(0)}_{1}\, \delta \overset{(2)}{\hat{u}}{}^{(0)}_{1} + \overset{(2)}{\ddot{w}}\, \delta \overset{(2)}{\hat{w}} \right]_{\overset{(2)}{x}_1=-l} \right\} \\
& - \frac{\overset{(2,3)}{M}}{2} \left\{ \left[\overset{(2)}{\ddot{u}}{}^{(0)}_{1}\, \delta \overset{(2)}{\hat{u}}{}^{(0)}_{1} + \overset{(2)}{\ddot{w}}\, \delta \overset{(2)}{\hat{w}} \right]_{\overset{(2)}{x}_1=l} + \left[\overset{(3)}{\ddot{u}}{}^{(0)}_{1}\, \delta \overset{(3)}{\hat{u}}{}^{(0)}_{1} + \overset{(3)}{\ddot{u}}{}^{(0)}_{2}\, \delta \overset{(3)}{\hat{u}}{}^{(0)}_{2} \right]_{\overset{(3)}{x}_1=-l} \right\} \\
& - \frac{\overset{(1,2)}{J}}{2} \left\{ \left[\overset{(1)}{\ddot{\chi}}\, \delta \overset{(1)}{\hat{\chi}} \right]_{\overset{(1)}{x}_2=\Theta} + \left[\overset{(2)}{\ddot{\phi}}\, \delta \overset{(2)}{\hat{\phi}} \right]_{\overset{(2)}{x}_1=-l} \right\} - \frac{\overset{(2,3)}{J}}{2} \left\{ \left[\overset{(2)}{\ddot{\phi}}\, \delta \overset{(2)}{\hat{\phi}} \right]_{\overset{(2)}{x}_1=l} + \left[\overset{(3)}{\ddot{\psi}}\, \delta \overset{(3)}{\hat{\psi}} \right]_{\overset{(3)}{x}_1=-l} \right\} \\
& + \delta \left[\overset{(1,2)}{\lambda}_{d} \left\{ \left[\overset{(1)}{\hat{u}}{}^{(0)}_{r} \right]_{\overset{(1)}{x}_2=\Theta} - \left[\overset{(2)}{\hat{w}} \right]_{\overset{(2)}{x}_1=-l} \right\} \right] + \delta \left[\overset{(1,2)}{\lambda}_{s} \left\{ \left[\overset{(1)}{\hat{\chi}} \right]_{\overset{(1)}{x}_2=\Theta} - \left[\overset{(2)}{\hat{\phi}} \right]_{\overset{(2)}{x}_1=-l} \right\} \right] \\
& + \delta \left[\overset{(1,2)}{\lambda}_{t} \left\{ \left[\overset{(1)}{\hat{u}}{}^{(0)}_{\theta} \right]_{\overset{(1)}{x}_2=\Theta} - \left[\overset{(2)}{\hat{u}}{}^{(0)}_{1} \right]_{\overset{(2)}{x}_1=-l} \right\} \right] + \delta \left[\overset{(2,3)}{\lambda}_{t} \left\{ \left[\overset{(2)}{\hat{u}}{}^{(0)}_{1} \right]_{\overset{(2)}{x}_1=l} - \left[\overset{(3)}{\hat{u}}{}^{(0)}_{1} \right]_{\overset{(3)}{x}_1=-l} \right\} \right] \\
& + \delta \left[\overset{(2,3)}{\lambda}_{d} \left\{ \left[\overset{(2)}{\hat{w}} \right]_{\overset{(2)}{x}_1=l} + \left[\overset{(3)}{\hat{u}}{}^{(0)}_{2} \right]_{\overset{(3)}{x}_1=-l} \right\} \right] + \delta \left[\overset{(2,3)}{\lambda}_{s} \left\{ \left[\overset{(2)}{\hat{\phi}} \right]_{\overset{(2)}{x}_1=l} + \left[\overset{(3)}{\hat{\psi}} \right]_{\overset{(3)}{x}_1=-l} \right\} \right] \Bigg] \Bigg] \Bigg] = 0, \qquad (17c)
\end{aligned}
$$

and

$$\overset{(1)}{\chi} \doteq \frac{1}{2}\left(\frac{\overset{(1)}{u}{}^{(0)}_{r,\theta}}{r} - \overset{(1)}{u}{}^{(0)}_{\theta,r} - \frac{\overset{(1)}{u}{}^{(0)}_{\theta}}{r}\right), \quad \overset{(2)}{\phi} \doteq \overset{(2)}{w}_{,1}, \quad \overset{(3)}{\psi} \doteq \frac{1}{2}\left(\overset{(3)}{u}{}^{(0)}_{2,1} - \overset{(3)}{u}{}^{(0)}_{1,2}\right). \tag{18}$$

Note that T_1^{IS}, T_2^{IS} and T_3^{IS} defined in Eqs. (17a)–(17c) are, respectively, the terms of the variational equation for the large surfaces, free opposing edges and interface and extreme edges of the structure for the vibration in the sensing direction in the absence of angular velocity.

Following the procedure used in the earlier treatment for the actuating motion of the configuration, the equivalent single point quantities for the sensing motion of the plates for both out-of-plane and in-plane displacements and slopes can be written in the form

$$\int_{R_i}^{R_o} \mathrm{d}\overset{(1)}{x}_1 \left[\overset{(1)}{\tau}{}^{(0)}_{\theta r}\, \delta\, \overset{(1)}{u}{}^{(0)}_{r}\right]_{\overset{(1)}{x}_2=\Theta} \doteq \left[\int_{R_i}^{R_o} \overset{(1)}{\tau}{}^{(0)}_{\theta r}\, \mathrm{d}\overset{(1)}{x}_1 \cdot \delta\, \hat{\overset{(1)}{u}}{}^{(0)}_{r}\right]_{\overset{(1)}{x}_2=\Theta}, \tag{19a}$$

$$\int_{R_i}^{R_o} \mathrm{d}\overset{(1)}{x}_1 \left[\overset{(1)}{\tau}{}^{(0)}_{\theta\theta}\, \delta\, \overset{(1)}{u}{}^{(0)}_{\theta}\right]_{\overset{(1)}{x}_2=\Theta} \doteq \left[\int_{R_i}^{R_o} \overset{(1)}{\tau}{}^{(0)}_{\theta\theta}\, \mathrm{d}\overset{(1)}{x}_1 \cdot \delta\, \hat{\overset{(1)}{u}}{}^{(0)}_{\theta} - \int_{R_i}^{R_o} \overset{(1)}{\tau}{}^{(0)}_{\theta\theta}(r-r_0)\, \mathrm{d}\overset{(1)}{x}_1 \cdot \delta\, \hat{\overset{(1)}{\chi}}\right]_{\overset{(1)}{x}_2=\Theta}, \tag{19b}$$

$$\int_{-b}^{b} \mathrm{d}\overset{(2)}{x}_2 \left[\left(\overset{(2)}{\tau}{}^{(0)}_{13} + \overset{(2)}{\tau}{}^{(1)}_{12,2}\right)\delta\, \overset{(2)}{w}\right]_{\overset{(2)}{x}_1=\pm l} \doteq \left[\int_{-b}^{b} \left(\overset{(2)}{\tau}{}^{(0)}_{13} + \overset{(2)}{\tau}{}^{(1)}_{12,2}\right) \mathrm{d}\overset{(2)}{x}_2 \cdot \delta\, \hat{\overset{(2)}{w}}\right]_{\overset{(2)}{x}_1=\pm l}, \tag{19c}$$

$$\int_{-b}^{b} \mathrm{d}\overset{(2)}{x}_2 \left[\overset{(2)}{\tau}{}^{(1)}_{11}\, \delta\, \overset{(2)}{\phi}\right]_{\overset{(2)}{x}_1=\pm l} \doteq \left[\int_{-b}^{b} \overset{(2)}{\tau}{}^{(1)}_{11}\, \mathrm{d}\overset{(2)}{x}_2 \cdot \delta\, \hat{\overset{(2)}{\phi}}\right]_{\overset{(2)}{x}_1=\pm l}, \tag{19d}$$

$$\int_{-b}^{b} \mathrm{d}\overset{(2)}{x}_2 \left[\overset{(2)}{\tau}{}^{(0)}_{11}\, \delta\, \overset{(2)}{u}{}^{(0)}_{1}\right]_{\overset{(2)}{x}_1=\pm l} \doteq \left[\int_{-b}^{b} \overset{(2)}{\tau}{}^{(0)}_{11}\, \mathrm{d}\overset{(2)}{x}_2 \cdot \delta\, \hat{\overset{(2)}{u}}{}^{(0)}_{1}\right]_{\overset{(2)}{x}_1=\pm l}, \tag{19e}$$

$$\int_{-b}^{b} \mathrm{d}\overset{(3)}{x}_2 \left[\overset{(3)}{\tau}{}^{(0)}_{11}\, \delta\, \overset{(3)}{u}{}^{(0)}_{1}\right]_{\overset{(3)}{x}_1=-l} \doteq \left[\int_{-b}^{b} \overset{(3)}{\tau}{}^{(0)}_{11}\, \mathrm{d}\overset{(3)}{x}_2 \cdot \delta\, \hat{\overset{(3)}{u}}{}^{(0)}_{1} - \int_{-b}^{b} \overset{(3)}{\tau}{}^{(0)}_{11}\, \overset{(3)}{x}_2\, \mathrm{d}\overset{(3)}{x}_2 \cdot \delta\, \hat{\overset{(3)}{\psi}}\right]_{\overset{(3)}{x}_1=-l}, \tag{19f}$$

$$\int_{-b}^{b} \mathrm{d}\overset{(3)}{x}_2 \left[\overset{(3)}{\tau}{}^{(0)}_{12}\, \delta\, \overset{(3)}{u}{}^{(0)}_{2}\right]_{\overset{(3)}{x}_1=-l} \doteq \left[\int_{-b}^{b} \overset{(3)}{\tau}{}^{(0)}_{12}\, \mathrm{d}\overset{(3)}{x}_2 \cdot \delta\, \hat{\overset{(3)}{u}}{}^{(0)}_{2}\right]_{\overset{(3)}{x}_1=-l}, \tag{19g}$$

where the first and second terms on the right-hand sides of Eqs. (19b) and (19f), respectively, represent the functionals for the symmetric and antisymmetric motions of the annular sector plate 1 and the rectangular plate 3, respectively, for the in-plane motion. For the sensing motion, the single point quantities for Kirchhoff's corner conditions may be

written in the form

$$\left[\overset{(2)}{\tau}{}^{(1)}_{12}\,\delta\,\overset{(2)}{w}\right]_{\overset{(2)}{x_1}=\pm l,\overset{(2)}{x_2}=\pm b} \doteq \left[\overset{(2)}{\tau}{}^{(1)}_{12}\,\delta\,\overset{(2)}{\hat{w}}\right]_{\overset{(2)}{x_1}=\pm l,\overset{(2)}{x_2}=\pm b}. \tag{19h}$$

Substituting the definitions of the equivalent point quantities (19a)–(19h) into the variational equation (16) and solving for the Lagrange multipliers as was done for the actuating motion, we obtain

$$\overset{(1,2)}{\lambda_d} = \frac{1}{2}\left[\left[\int_{R_i}^{R_o} \overset{(1)}{\tau}{}^{(0)}_{\theta r}\,\mathrm{d}\,\overset{(1)}{x_1}\right]_{\overset{(1)}{x_2}=\Theta} + \left[\int_{-b}^{b}\left(\overset{(2)}{\tau}{}^{(0)}_{13} + \overset{(2)}{\tau}{}^{(0)}_{12,2}\right)\mathrm{d}\,\overset{(2)}{x_2}\right]_{\overset{(2)}{x_1}=-l} - \left[\overset{(2)}{\tau}{}^{(1)}_{12}\right]_{\overset{(2)}{x_1}=-l,\overset{(2)}{x_2}=-b}^{\overset{(2)}{x_1}=-l,\overset{(2)}{x_2}=b} + \frac{\overset{(1,2)}{M}}{2}\left\{\left[\overset{(1)}{\ddot{u}}{}^{(0)}_{r}\right]_{\overset{(1)}{x_2}=\Theta} - \left[\overset{(2)}{\ddot{w}}\right]_{\overset{(2)}{x_1}=-l}\right\}\right], \tag{20a}$$

$$\overset{(1,2)}{\lambda_s} = \frac{1}{2}\left[-\left[\int_{R_i}^{R_o} \overset{(1)}{\tau}{}^{(0)}_{\theta\theta}(r-r_0)\,\mathrm{d}\,\overset{(1)}{x_1}\right]_{\overset{(1)}{x_2}=\Theta} - \left[\int_{-b}^{b} \overset{(2)}{\tau}{}^{(1)}_{11}\,\mathrm{d}\,\overset{(2)}{x_2}\right]_{\overset{(2)}{x_1}=-l} + \frac{\overset{(1,2)}{J}}{2}\left\{\left[\overset{(1)}{\ddot{\chi}}\right]_{\overset{(1)}{x_2}=\Theta} - \left[\overset{(2)}{\ddot{\phi}}\right]_{\overset{(2)}{x_1}=-l}\right\}\right], \tag{20b}$$

$$\overset{(1,2)}{\lambda_t} = \frac{1}{2}\left[-\left[\int_{R_i}^{R_o} \overset{(1)}{\tau}{}^{(0)}_{\theta\theta}\,\mathrm{d}\,\overset{(1)}{x_1}\right]_{\overset{(1)}{x_2}=\Theta} + \left[\int_{-b}^{b} \overset{(2)}{\tau}{}^{(0)}_{11}\,\mathrm{d}\,\overset{(2)}{x_2}\right]_{\overset{(2)}{x_1}=-l} + \frac{\overset{(1,2)}{M}}{2}\left\{\left[\overset{(1)}{\ddot{u}}{}^{(0)}_{\theta}\right]_{\overset{(1)}{x_2}=\Theta} - \left[\overset{(2)}{\ddot{u}}{}^{(0)}_{1}\right]_{\overset{(2)}{x_1}=-l}\right\}\right], \tag{20c}$$

$$\overset{(2,3)}{\lambda_t} = \frac{1}{2}\left[\left[\int_{-b}^{b} \overset{(2)}{\tau}{}^{(0)}_{11}\,\mathrm{d}\,\overset{(2)}{x_2}\right]_{\overset{(2)}{x_1}=l} + \left[\int_{-b}^{b} \overset{(3)}{\tau}{}^{(0)}_{11}\,\mathrm{d}\,\overset{(3)}{x_2}\right]_{\overset{(3)}{x_1}=-l} + \frac{\overset{(2,3)}{M}}{2}\left\{\left[\overset{(2)}{\ddot{\hat{u}}}{}^{(0)}_{1}\right]_{\overset{(2)}{x_1}=l} - \left[\overset{(3)}{\ddot{\hat{u}}}{}^{(0)}_{1}\right]_{\overset{(3)}{x_1}=-l}\right\}\right], \tag{20d}$$

$$\overset{(2,3)}{\lambda_d} = \frac{1}{2}\left[\left[\int_{-b}^{b}\left(\overset{(2)}{\tau}{}^{(0)}_{13} + \overset{(2)}{\tau}{}^{(1)}_{12,2}\right)\mathrm{d}\,\overset{(2)}{x_2}\right]_{\overset{(2)}{x_1}=l} - \left[\overset{(2)}{\tau}{}^{(1)}_{12}\right]_{\overset{(2)}{x_1}=-l,\overset{(2)}{x_2}=-b}^{\overset{(2)}{x_1}=-l,\overset{(2)}{x_2}=b} - \left[\int_{-b}^{b} \overset{(3)}{\tau}{}^{(0)}_{12}\,\mathrm{d}\,\overset{(3)}{x_2}\right]_{\overset{(3)}{x_1}=-l} + \frac{\overset{(2,3)}{M}}{2}\left\{\left[\overset{(2)}{\ddot{w}}\right]_{\overset{(2)}{x_1}=l} + \left[\overset{(3)}{\ddot{u}}{}^{(0)}_{2}\right]_{\overset{(3)}{x_1}=-l}\right\}\right], \tag{20e}$$

$$\overset{(2,3)}{\lambda_s} = \frac{1}{2}\left[-\left[\int_{-b}^{b} \overset{(2)}{\tau}{}^{(1)}_{11}\, \mathrm{d}\overset{(2)}{x}_2\right]_{\overset{(2)}{x_1}=l} + \left[\int_{-b}^{b} \overset{(3)}{\tau}{}^{(0)}_{11}\, \overset{(3)}{x}_2\, \mathrm{d}\overset{(3)}{x}_2\right]_{\overset{(3)}{x_1}=-l} + \frac{\overset{(2,3)}{J}}{2}\left\{ \left[\overset{(2)}{\ddot{\hat{\phi}}}\right]_{\overset{(2)}{x_1}=l} + \left[\overset{(3)}{\ddot{\hat{\psi}}}\right]_{\overset{(3)}{x_1}=-l} \right\} \right]. \tag{20f}$$

2.5. Two-dimensional constitutive equations including coupling with electric properties for the bimorph plates

The three-dimensional constitutive equations relating the elastic field tensors (stress tensor τ_{ij} and strain tensor ε_{ij}) and the electric field vectors (electric field E_k and electric displacement D_i) can be expressed with the following pair of piezoelectric equations in compressed notation [21]:

$$\tau_p = c^E_{pq}\varepsilon_q - e_{kp}E_k, \quad D_i = e_{iq}\varepsilon_q + \varepsilon^S_{ik}E_k, \tag{21}$$

where the indices $i,\ k$ range over $1, 2, 3$ whereas p, q range over $1, 2, \ldots, 6$.

For the material having C_{6v}(6 mm) symmetry [21], the elastic and piezoelectric constants as well as the dielectric constants as matrices can be written in the form

$$c^E_{pq} = \begin{bmatrix} c^E_{11} & c^E_{12} & c^E_{13} & 0 & 0 & 0 \\ c^E_{12} & c^E_{11} & c^E_{13} & 0 & 0 & 0 \\ c^E_{13} & c^E_{13} & c^E_{33} & 0 & 0 & 0 \\ 0 & 0 & 0 & c^E_{44} & 0 & 0 \\ 0 & 0 & 0 & 0 & c^E_{44} & 0 \\ 0 & 0 & 0 & 0 & 0 & c_{66} \end{bmatrix}, \quad e_{ip} = \begin{bmatrix} 0 & 0 & 0 & 0 & e_{15} & 0 \\ 0 & 0 & 0 & e_{15} & 0 & 0 \\ e_{31} & e_{31} & e_{33} & 0 & 0 & 0 \end{bmatrix}, \quad \varepsilon^S_{ij} = \begin{bmatrix} \varepsilon^S_{11} & 0 & 0 \\ 0 & \varepsilon^S_{11} & 0 \\ 0 & 0 & \varepsilon^S_{33} \end{bmatrix}, \tag{22}$$

$$c_{66} = (c^E_{11} - c^E_{12})/2,$$

where the piezoceramic material is polarized along the x_3 direction. Note that the total number of independent material constants for the C_{6v} class is 10. For convenience, Eqs. (21) with (22) are written out here in the form

$$\tau_1 = c^E_{11}\varepsilon_1 + c^E_{12}\varepsilon_2 + c^E_{13}\varepsilon_3 - e_{31}E_3, \tag{23a}$$

$$\tau_2 = c^E_{12}\varepsilon_1 + c^E_{11}\varepsilon_2 + c^E_{13}\varepsilon_3 - e_{31}E_3, \tag{23b}$$

$$\tau_3 = c^E_{13}\varepsilon_1 + c^E_{13}\varepsilon_2 + c^E_{33}\varepsilon_3 - e_{33}E_3, \tag{23c}$$

$$\tau_4 = c^E_{44}\varepsilon_4 - e_{15}E_2, \quad \tau_5 = c^E_{44}\varepsilon_5 - e_{15}E_1, \quad \tau_6 = c_{66}\varepsilon_6, \tag{23d–f}$$

$$D_1 = e_{15}\varepsilon_5 + \varepsilon^S_{11}E_1, \quad D_2 = e_{15}\varepsilon_4 + \varepsilon^S_{11}E_2, \tag{23g, h}$$

$$D_3 = e_{31}(\varepsilon_1 + \varepsilon_2) + e_{33}\varepsilon_3 + \varepsilon^S_{33}E_3. \tag{23i}$$

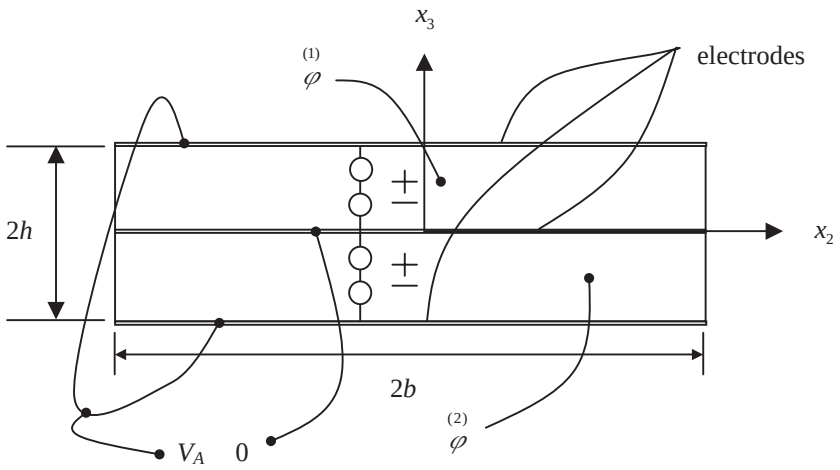

Fig. 3. Cross-sectional view of a fully electroded bimorph plate.

In the case of plane stress $\tau_3 = 0$, we may solve Eq. (23c) for ε_3 with $\tau_3 = 0$ and substitute into Eqs. (23a), (23b) and (23i) to obtain

$$\tau_1 = c_{11}^{E^*}(\varepsilon_1 + \hat{\nu}\varepsilon_2) - e_{31}^{*}E_3, \tag{24}$$

$$\tau_2 = c_{11}^{E^*}(\varepsilon_2 + \hat{\nu}\varepsilon_1) - e_{31}^{*}E_3, \tag{25}$$

$$D_3 = e_{31}^{*}(\varepsilon_1 + \varepsilon_2) + \varepsilon_{33}^{S^*}E_3, \tag{26}$$

where

$$c_{11}^{E^*} = c_{11}^{E} - c_{13}^{E^2}/c_{33}^{E}, \quad c_{12}^{E^*} = c_{12}^{E} - c_{13}^{E^2}/c_{33}^{E}, \quad \hat{\nu} = c_{12}^{E^*}/c_{11}^{E^*} \tag{27a}$$

and

$$e_{31}^{*} = e_{31} - c_{13}^{E}e_{33}/c_{33}^{E}, \quad \varepsilon_{33}^{S^*} = \varepsilon_{33}^{S} + e_{33}^{2}/c_{33}^{E}. \tag{27b}$$

Consider a bimorph plate with fully electroded surfaces normal to x_3 for each plate on which electric potentials are prescribed. A cross-sectional view of the symmetric bimorph plate with fully electroded surfaces is shown in Fig. 3. In this figure, the plate is polarized along the x_3 axis, the total thickness is $2h$ and total width is $2b$, and infinitesimally thin electrodes are attached to the top, bottom and inserted in the middle. Here, the superscripts in the middle denote the layers, i.e., $\langle 1 \rangle$ for the upper layer and $\langle 2 \rangle$ for the lower layer. Since the thickness of the bimorph plate is assumed to be much thinner than the other dimensions, it is convenient to write the equation of electrostatics for each piezoelectric portion of the bimorph

in the form

$$\overset{\langle m\rangle}{D}_{1,1} + \overset{\langle m\rangle}{D}_{2,2} + \overset{\langle m\rangle}{D}_{3,3} = 0, \quad m = 1, 2. \tag{28}$$

Since the bimorph is thin and there are complete electrodes on the horizontal surfaces mentioned, we may take

$$\overset{\langle m\rangle}{E}_1 = 0, \quad \overset{\langle m\rangle}{E}_2 = 0, \quad m = 1, 2 \tag{29}$$

throughout the bimorph. Since the shearing strain ε_4 and ε_5 are neglected in classical flexure, from Eqs. (23g) and (23h) with Eq. (29), we have

$$\overset{\langle m\rangle}{D}_1 = \overset{\langle m\rangle}{D}_2 = 0, \quad m = 1, 2 \tag{30}$$

throughout the bimorph. From Eqs. (28) and (30), we find that the equation of electrostatics for the bimorph takes the form

$$\overset{\langle m\rangle}{D}_{3,3} = 0, \quad m = 1, 2. \tag{31}$$

An important consequence of Eqs. (29)–(31) is that the purely elastic solutions obtained for the orthotropic material in Refs. [11,13–15] are applicable to the piezoelectric case treated in this work provided only that the flexural constants are modified by the influence of the piezoelectric coupling as shown in Eqs. $(43)_2$, $(43)_3$ and (45) below. In the case of in-plane motion the influence of the piezoelectric coupling cancels in the bimorph.

Since in classical flexure the three-dimensional strains ε_1 and ε_2 in Eq. (26) are linear functions of x_3, from Eqs. (26) and (31), we find that E_3 in the bimorph must be of the form

$$\overset{\langle m\rangle}{E}_3 = \overset{\langle m\rangle}{E}_3^{(0)} + x_3 \overset{\langle m\rangle}{E}_3^{(1)}, \quad m = 1, 2, \tag{32}$$

where $\overset{\langle m\rangle}{E}_3^{(0)}$ and $\overset{\langle m\rangle}{E}_3^{(1)}$ are independent of x_3. In quasielectrostatics, E_i is given by

$$\overset{\langle m\rangle}{E}_i = -\overset{\langle m\rangle}{\varphi}_{,i}, \quad m = 1, 2, \tag{33}$$

where $\overset{\langle m\rangle}{\varphi}$ is the electric potential in the mth layer. From Eqs. (32) and (33), we must have

$$\overset{\langle m\rangle}{\varphi} = x_3 \overset{\langle m\rangle}{\varphi}^{(1)} + x_3^2 \overset{\langle m\rangle}{\varphi}^{(2)}, \quad m = 1, 2, \tag{34}$$

for each region of the bimorph since the lowest order expansion in electric potential is completely adequate for the fully electroded piezoelectric bimorph.[7] Furthermore, from Eqs. (29) and (34)

[7] Higher order expansions in electric potential may be obtained by including additional terms in Eq. (34), each of which must vanish at each electrode. When this is done two-dimensional electrostatic plate equations are obtained by means of the $\aleph_e$ term in Eqs. (2) and (4). Although it was implied in Section 2.1 that this would be done, it is not going

$\overset{\langle m\rangle}{\varphi}{}^{(1)}$ and $\overset{\langle m\rangle}{\varphi}{}^{(2)}$ must be independent of x_1 and x_2.

From the electric boundary conditions shown in Fig. 3 and Eqs. (34), we obtain

$$\overset{\langle 1\rangle}{\varphi}{}^{(1)} = \frac{1}{h}\left(V_A(t) - h^2\,\overset{\langle 1\rangle}{\varphi}{}^{(2)}\right), \quad \overset{\langle 2\rangle}{\varphi}{}^{(1)} = -\frac{1}{h}\left(V_A(t) - h^2\,\overset{\langle 2\rangle}{\varphi}{}^{(2)}\right). \tag{35}$$

The substitution of Eq. (34) into Eq. (33) yields

$$\overset{\langle m\rangle}{E}_3 = -\overset{\langle m\rangle}{\varphi}{}^{(1)} - 2x_3\,\overset{\langle m\rangle}{\varphi}{}^{(2)}, \quad m = 1, 2, \tag{36}$$

in conformity with Eq. (32). Substituting Eq. (34) into Eq. (31), along with Eqs. (26), (36) and the first two of the flexural strain relations

$$\varepsilon_1 = x_3\varepsilon_1^{(1)}, \quad \varepsilon_2 = x_3\varepsilon_2^{(1)}, \quad \varepsilon_6 = x_3\varepsilon_6^{(1)}, \tag{37}$$

in Mindlin's notation [12], we obtain

$$\overset{\langle m\rangle}{D}_{3,3} = e_{31}^*(\varepsilon_1^{(1)} + \varepsilon_2^{(1)}) - 2\varepsilon_{33}^{S*}\,\overset{\langle m\rangle}{\varphi}{}^{(2)} = 0, \quad m = 1, 2, \tag{38}$$

which yield

$$\overset{\langle m\rangle}{\varphi}{}^{(2)} = \frac{e_{31}^*(\varepsilon_1^{(1)} + \varepsilon_2^{(1)})}{2\varepsilon_{33}^{S*}}, \quad m = 1, 2. \tag{39}$$

Substituting Eqs. (35) and (39) into Eq. (34), we obtain the electric potentials

$$\overset{\langle 1\rangle}{\varphi} = \left\{\frac{V_A(t)}{h} - \frac{e_{31}^* h}{2\varepsilon_{33}^{S*}}(\varepsilon_1^{(1)} + \varepsilon_2^{(1)})\right\}x_3 + \frac{e_{31}^*}{2\varepsilon_{33}^{S*}}(\varepsilon_1^{(1)} + \varepsilon_2^{(1)})x_3^2, \tag{40a}$$

$$\overset{\langle 2\rangle}{\varphi} = -\left\{\frac{V_A(t)}{h} - \frac{e_{31}^* h}{2\varepsilon_{33}^{S*}}(\varepsilon_1^{(1)} + \varepsilon_2^{(1)})\right\}x_3 + \frac{e_{31}^*}{2\varepsilon_{33}^{S*}}(\varepsilon_1^{(1)} + \varepsilon_2^{(1)})x_3^2 \tag{40b}$$

and from Eq. (33) the electric fields

$$\overset{\langle 1\rangle}{E}_3 = -\left\{\frac{V_A(t)}{h} - \frac{e_{31}^* h}{2\varepsilon_{33}^{S*}}(\varepsilon_1^{(1)} + \varepsilon_2^{(1)})\right\} - \frac{e_{31}^*}{\varepsilon_{33}^{S*}}(\varepsilon_1^{(1)} + \varepsilon_2^{(1)})x_3, \tag{41a}$$

$$\overset{\langle 2\rangle}{E}_3 = \left\{\frac{V_A(t)}{h} - \frac{e_{31}^* h}{2\varepsilon_{33}^{S*}}(\varepsilon_1^{(1)} + \varepsilon_2^{(1)})\right\} - \frac{e_{31}^*}{\varepsilon_{33}^{S*}}(\varepsilon_1^{(1)} + \varepsilon_2^{(1)})x_3. \tag{41b}$$

(*footnote continued*)
to be included in this work because it results in unwarranted additional complications in the description, all of which will be excluded before any problem is treated since, as already noted in the text, the lowest order expansion in electric potential is completely adequate for the fully electroded piezoelectric bimorph.

The substitution of Eqs. (41a) and (41b), along with Eqs. $(37)_{1,2}$, into Eqs. (24) and (25) yields the bending moment and strain component relations in the form

$$\tau_1^{(1)} = \int_0^h {}^{\langle 1\rangle}\tau_1\, x_3\, \mathrm{d}x_3 + \int_{-h}^0 {}^{\langle 2\rangle}\tau_1\, x_3\, \mathrm{d}x_3 = \hat{K}V_A(t) + \bar{\bar{D}}(\varepsilon_1^{(1)} + \bar{\bar{\nu}}\varepsilon_2^{(1)}), \tag{42a}$$

$$\tau_2^{(1)} = \int_0^h {}^{\langle 1\rangle}\tau_2\, x_3\, \mathrm{d}x_3 + \int_{-h}^0 {}^{\langle 2\rangle}\tau_2\, x_3\, \mathrm{d}x_3 = \hat{K}V_A(t) + \bar{\bar{D}}(\varepsilon_2^{(1)} + \bar{\bar{\nu}}\varepsilon_1^{(1)}), \tag{42b}$$

where

$$\hat{K} = e_{31}^* h, \quad \bar{\bar{D}} = \frac{2h^3}{3}\left(c_{11}^{E^*} + \frac{e_{31}^{*2}}{4\varepsilon_{33}^{S^*}}\right), \quad \bar{\bar{\nu}} = \frac{4c_{11}^{E^*}\hat{\nu} + e_{31}^{*2}/\varepsilon_{33}^{S^*}}{4c_{11}^{E^*} + e_{31}^{*2}/\varepsilon_{33}^{S^*}}, \tag{43}$$

and we note that $\bar{\bar{D}}$ and $\bar{\bar{\nu}}$ are the flexural constants modified by the piezoelectric coupling. It should be noted that Eqs. (42) obtained for the bimorph are equivalent to the results presented in Section 6 of Ref. [9] and Section 12 of Ref. [10]. In the case of in-plane motion, the expressions equivalent to Eqs. (41a) and (41b) when substituted in Eqs. (24) and (25) reveal that the influence of the piezoelectric coupling cancels in the bimorph.

As stated earlier, the bending moments $\tau_1^{(1)}$ and $\tau_2^{(1)}$ of the bimorph plate have the forcing terms $\hat{K}V_A(t)$ induced by an externally applied voltage in addition to the flexural terms, as can be seen in Eqs. (42a) and (42b).

From Eqs. (23f) and $(37)_3$, we also obtain the relation between the twisting moment and strain component in the form

$$\tau_6^{(1)} = \int_{-h}^h \tau_6 x_3\, \mathrm{d}x_3 = \hat{D}\varepsilon_6^{(1)}, \tag{44}$$

where

$$\hat{D} = 2h^3 c_{66}/3, \tag{45}$$

which shows that the piezoelectric coupling has no influence on $\hat{D}$.

The introduction of the strain–deflection relations (7) of Refs. [11] into Eqs. (42a), (42b) and (44) yields the moment–plate curvature relations for the rectangular bimorph plate in the form

$$\tau_{11}^{(1)} = \hat{K}V_A(t) - \bar{\bar{D}}(w_{,11} + \bar{\bar{\nu}}w_{,22}), \quad \tau_{22}^{(1)} = \hat{K}V_A(t) - \bar{\bar{D}}(w_{,22} + \bar{\bar{\nu}}w_{,11}), \tag{46a}$$

$$\tau_{12}^{(1)} = -2\bar{\bar{D}}r_D w_{,12}, \tag{46b}$$

where

$$r_D = \hat{D}/\bar{\bar{D}}. \tag{47}$$

The substitution of Eqs. $(22)_4$, $(43)_{2,3}$ and (45) into Eq. (47) simply yields

$$r_D = \frac{(1-\bar{\bar{\nu}})}{2}, \tag{48}$$

since the material has hexagonal symmetry.

Since the plate shearing strains are neglected in classical flexure, we may ignore the constitutive equations for $\tau_4^{(0)}$ and $\tau_5^{(0)}$ and use Eq. (17b) of Ref. [11] instead, i.e.,

$$\tau_{3b}^{(0)} = \tau_{ab,a}^{(1)}. \tag{49}$$

The substitution of Eqs. (46a), (46b), (48) and (49) into Kirchhoff's strain–twist equations yields

$$\tau_{31}^{(0)} + \tau_{12,2}^{(1)} = -\bar{\hat{D}}\{w_{,111} + (2-\bar{\hat{\nu}})w_{,122}\}, \quad \tau_{32}^{(0)} + \tau_{12,1}^{(1)} = -\bar{\hat{D}}\{w_{,222} + (2-\bar{\hat{\nu}})w_{,211}\}, \tag{50}$$

in terms of the bimorph deflection.

For the flexural vibration of the annular sector plate with shorted electrodes, the stress resultant–plate deflection relations given in Eqs. (13)–(15) and (19), (20) in Ref. [14] with $R = 1, T = 1$, and with the respective replacements of $\hat{D}, \hat{\nu}$ with $\bar{\hat{D}}$, $\bar{\hat{\nu}}$, take the form

$$\tau_{rr}^{(1)} = -\bar{\hat{D}}\left\{v_{,rr} + \frac{\bar{\hat{\nu}}}{r}\left(v_{,r} + \frac{v_{,\theta\theta}}{r}\right)\right\}, \quad \tau_{\theta\theta}^{(1)} = -\bar{\hat{D}}\left\{\bar{\hat{\nu}}v_{,rr} + \frac{1}{r}\left(v_{,r} + \frac{v_{,\theta\theta}}{r}\right)\right\}, \tag{51}$$

$$\tau_{r\theta}^{(1)} = -\bar{\hat{D}}(1-\bar{\hat{\nu}})(v/r)_{,r\theta}, \tag{52}$$

$$\tau_{rz}^{(0)} + \frac{1}{r}\frac{\partial\tau_{r\theta}^{(1)}}{\partial\theta} = -\bar{\hat{D}}\left\{v_{,rrr} - \frac{v_{,r}}{r^2} + \frac{v_{,rr}}{r} - \frac{v_{,\theta\theta}}{r^3} + \frac{(2-\bar{\hat{\nu}})}{r^2}\left(v_{,r\theta\theta} - \frac{v_{,\theta\theta}}{r}\right)\right\}, \tag{53}$$

$$\tau_{\theta z}^{(0)} + \frac{\partial\tau_{\theta r}^{(1)}}{\partial r} = -\bar{\hat{D}}\left\{\frac{v_{,\theta\theta\theta}}{r^3} - \frac{v_{,r\theta}}{r^2} + \frac{2}{r}\left(v_{,rr\theta} + \frac{v_{,\theta}}{r^2}\right) - \bar{\hat{\nu}}\left(\frac{v_{,rr\theta}}{r} + \frac{2v_{,\theta}}{r^3} - \frac{2v_{,r\theta}}{r^2}\right)\right\}. \tag{54}$$

Furthermore, with $R = 1$ and with the respective replacements of c_{11}^*, c_{12}^* with $c_{11}^{E^*}$, $c_{12}^{E^*}$, Eqs. (3), (4) in Ref. [13] can also be used for the in-plane motions of the rectangular plate:

$$\tau_{11}^{(0)} = 2hc_{11}^{E^*}(u_{1,1}^{(0)} + \hat{\nu}u_{2,2}^{(0)}), \quad \tau_{22}^{(0)} = 2hc_{11}^{E^*}(u_{2,2}^{(0)} + \hat{\nu}u_{1,1}^{(0)}), \tag{55}$$

$$\tau_{12}^{(0)} = 2hc_{66}(u_{1,2}^{(0)} + u_{2,1}^{(0)}) \tag{56}$$

and Eqs. (12)–(14) in Ref. [15] for the in-plane motions of the annular sector plate:

$$\tau_{rr}^{(0)} = 2hc_{11}^{E^*}\left\{u_{r,r}^{(0)} + \frac{\hat{\nu}}{r}(u_{\theta,\theta}^{(0)} + u_r^{(0)})\right\}, \quad \tau_{\theta\theta}^{(0)} = 2hc_{11}^{E^*}\left\{\hat{\nu}u_{r,r}^{(0)} + \frac{1}{r}(u_{\theta,\theta}^{(0)} + u_r^{(0)})\right\}, \tag{57}$$

$$\tau_{r\theta}^{(0)} = 2hc_{66}\left\{\frac{u_{r,\theta}^{(0)}}{r} + r\left(\frac{u_\theta^{(0)}}{r}\right)_{,r}\right\}. \tag{58}$$

Eqs. (46a), (46b), (50) and (55), (56) are, respectively, the stress resultant–deflection relations required for flexural vibrations and in-plane stress–displacement gradient relations for the rectangular bimorph plates, and Eqs. (51)–(54) and (57), (58) are, respectively, the stress resultant–deflection relations required for the flexural vibrations and in-plane stress–displacement gradient relations for the annular sector bimorph plate.

2.6. Relations between electric current and plate deflections

Through the use of Eqs. (26), (41a) and (41b), we obtain the electric displacement in the x_3 direction at the top and bottom surfaces in the form

$$\overset{\langle 1\rangle}{D}_3(h) = -\frac{1}{h}\left[\varepsilon_{33}^{S^*} V_A(t) - \frac{e_{31}^* h^2}{2}(\varepsilon_1^{(1)} + \varepsilon_2^{(1)})\right], \tag{59a}$$

$$\overset{\langle 2\rangle}{D}_3(-h) = \frac{1}{h}\left[\varepsilon_{33}^{S^*} V_A(t) - \frac{e_{31}^* h^2}{2}(\varepsilon_1^{(1)} + \varepsilon_2^{(1)})\right]. \tag{59b}$$

Using Eqs. (59a) and (59b), after introducing the strain–displacement relations described in Eq. (7) of Ref. [11], we obtain the relations between the electric current, the applied voltage and the deflection of the plate with the result

$$\begin{aligned}\overset{\langle m\rangle}{I}_A &= -\int_{S_A} \overset{\langle 1\rangle}{\dot{D}}_3(h)\,\mathrm{d}S = \int_{S_A} \overset{\langle 2\rangle}{\dot{D}}_3(-h)\,\mathrm{d}S \\ &= \frac{\mathrm{i}\omega}{h}\left[\varepsilon_{33}^{S^*} V_A S_A + \frac{e_{31}^* h^2}{2}\int_{S_A}(w_{,11} + w_{,22})\,\mathrm{d}S\right], \quad m = 1, 2,\end{aligned} \tag{60}$$

where S_A is the surface area of the actuating plate and we have followed the convention of Ref. [22]. Note that the first term in the right-hand side of Eq. (60) represents the current due to the applied voltage and the second term represents the current due to the mechanical motion.

If the subscript A in Eq. (60) is changed to S, the equation holds for the sensing plate. If in the resulting equation V_S is set equal to zero, the short-circuit current is obtained in the form

$$\begin{aligned}\overset{\langle m\rangle}{I}_S &= -\int_{S_S} \overset{\langle 1\rangle}{\dot{D}}_3(h)\,\mathrm{d}S = \int_{S_S} \overset{\langle 2\rangle}{\dot{D}}_3(-h)\,\mathrm{d}S \\ &= \mathrm{i}\omega\frac{e_{31}^* h}{2}\int_{S_S}(w_{,11} + w_{,22})\,\mathrm{d}S, \quad m = 1, 2.\end{aligned} \tag{61}$$

It should be noted that Eqs. (60) and (61) give the same result as in Section 6 of Ref. [9].

For future usage, we define the sensitivity S here in the form

$$S \doteq \left|\overset{\langle m\rangle}{I}_S\right| \Big/ \left|\overset{\langle m\rangle}{I}_A\right|, \quad m = 1, 2. \tag{62}$$

It is important to note that both the actuating and the sensing plates have been treated as passive elements in this description.

3. Implications of analysis

In this work, a dynamic analysis for a resonator arranged in the shape of one half of a single tuning fork with polarized piezoceramic bimorphs has been presented. Since the geometric configuration is very complex, simplification of the modelling procedure needs to be taken into account. We have developed a variational approximation procedure for the dynamic analysis of the tuning fork shown in Fig. 1. Since the thin plates are joined at right angles, equivalent point quantities have been defined at the junctions in order to obtain the interface conditions. This

modelling procedure provides a convenient means of investigating the dynamic characteristics of the complicated resonator configuration treated in this work.

This modelling effort represents the first attempt to describe the tuning fork gyroscope system considered in this work, which is a very complicated configuration and is coupled to the electrical properties. The analytical method presented is very useful for obtaining the solutions for the free and forced vibrations of the foregoing tuning fork. The superposed angular velocity is included in the companion paper [23], along with detailed calculations.

References

[1] L. Foucault, *Travaux Scientifiques de Foucault*, Paris, 1878.
[2] R.E. Barnaby, J.B. Chatterton, F.H. Gerring, General theory and operational characteristics of the Gyrotron angular rate tachometer, *Aeronautical Engineering Review* 12 (11) (1953) 31–36.
[3] W.D. Gates, Vibrating angular rate sensor may threaten the gyroscope, *Electronics* 41 (10) (1968) 130–134.
[4] J. Söderkvist, Micromachined gyroscopes, *Sensors and Actuators* 43 (1994) 65–71.
[5] W.S. Watson, Angular rate sensor apparatus, US Patent No. 4,628,734, 1986.
[6] S. Kudo, M. Konno, S. Sugawara, T. Yoshida, Vibrational analysis of tuning fork gyroscope with orthogonal vibration arms, *Japanese Journal of Applied Physics* 32 (1993) 2310–2313.
[7] S. Kudo, M. Konno, S. Sugawara, T. Yoshida, Finite element analysis of H-type vibratory gyroscope, *Japanese Journal of Applied Physics* 31 (1992) 3257–3260.
[8] I.A. Ulitko, Mathematical theory of the fork-type wave gyroscope, *IEEE International Frequency Control Symposium*, IEEE, Piscataway, NJ, 1995, pp. 786–793.
[9] D.H. Keuning, Approximate equations for the flexure of thin, incomplete, piezoelectric bimorphs, *Journal of Engineering Mathematics* 5 (4) (1971) 307–319.
[10] N.N. Rogacheva, *The Theory of Piezoelectric Shells and Plates*, CRC Press, London, 1994.
[11] Jongwon Seok, H.F. Tiersten, H.A. Scarton, Free vibrations of rectangular cantilever plates. Part 1: out-of-plane motion, *Journal of Sound and Vibration* 271 (1–2) (2004) 131–146.
[12] R.D. Mindlin, *An Introduction to the Mathematical Theory of the Vibration of Elastic Plates*, US Army Signal Corps Engineering Laboratory, Fort Monmouth, NJ, 1955, Section 6.04.
[13] Jongwon Seok, H.F. Tiersten, H.A. Scarton, Free vibrations of rectangular cantilever plates. Part 2: in-plane motion, *Journal of Sound and Vibration* 271 (1–2) (2004) 147–158.
[14] Jongwon Seok, H.F. Tiersten, Free vibrations of annular sector cantilever plates. Part 1: out-of-plane motion, *Journal of Sound and Vibration* 271 (3–5) (2004) 757–772.
[15] Jongwon Seok, H.F. Tiersten, Free vibrations of annular sector cantilever plates. Part 2: in-plane motion, *Journal of Sound and Vibration* 271 (3–5) (2004) 773–787.
[16] C. Lanczos, *The Variational Principles of Mechanics*, University of Toronto Press, Toronto, 1949, Section 6 (Chapter I).
[17] H.F. Tiersten, *Linear Piezoelectric Plate Vibrations*, Plenum Press, New York, 1969 Section 6.2.
[18] H.F. Tiersten, *Linear Piezoelectric Plate Vibrations*, Plenum Press, New York, 1969 Sections 6.2–6.3.
[19] H.F. Tiersten, *Linear Piezoelectric Plate Vibrations*, Plenum Press, New York, 1969 Section 6.4.
[20] F.B. Hildebrand, *Methods of Applied Mathematics*, 2nd Edition, Prentice-Hall, Englewood Cliffs, NJ, 1965, p. 219, Problem 100.
[21] H.F. Tiersten, *Linear Piezoelectric Plate Vibrations*, Plenum Press, New York, 1969 Section 7.1.
[22] H.H. Skilling, Electric current is considered positive if it flows from active to passive + to +, *Electrical Engineering Circuits*, Wiley, New York, 1959.
[23] Jongwon Seok, H.F. Tiersten, H.A. Scarton, An analysis of a vibratory angular-rate gyroscope using polarized piezoceramic bimorph plates. Part 2: solution procedure for the gyroscope with superposed angular velocity, *Journal of Sound and Vibration* 280 (1–2) (2005) 289–310.